Cooperative DnaA Binding to the Negatively Supercoiled datA Locus Stimulates DnaA-ATP Hydrolysis

Kasho, Kazutoshi
Department of Molecular Biology, Graduate School of Pharmaceutical Sciences, Kyushu University

Tanaka, Hiroyuki
Department of Molecular Biology, Graduate School of Pharmaceutical Sciences, Kyushu University | Hisamitsu Pharmaceutical Co.

Sakai, Ryuji
Department of Molecular Biology, Graduate School of Pharmaceutical Sciences, Kyushu University

Katayama, Tsutomu
Department of Molecular Biology, Graduate School of Pharmaceutical Sciences, Kyushu University

出版情報：Journal of Biological Chemistry, pp.1-, 2017-01-27
バージョン：
権利関係：

Cooperative DnaA binding to the negatively supercoiled *datA* locus stimulates DnaA-ATP hydrolysis

Kazutoshi Kasho[1], Hiroyuki Tanaka[1,2], Ryuji Sakai[1], and Tsutomu Katayama[1]

[1]Department of Molecular Biology, Graduate School of Pharmaceutical Sciences, Kyushu University, Fukuoka 812-8582, Japan. [2]Present address: Hisamitsu Pharmaceutical Co., Tosu, Saga, 841-0017, Japan.

Running title: *Mechanism of DnaA-ATP hydrolysis by supercoiled* datA

To whom correspondence should be addressed: Tsutomu Katayama, Department of Molecular Biology, Graduate School of Pharmaceutical Sciences, Kyushu University, Fukuoka 812-8582, Japan., Tel. +81-92-642-6641; Fax +81-92-642-6646; E-mail katayama@phar.kyushu-u.ac.jp

Keywords: DNA binding protein; DNA replication; DNA topology; DNA-protein interaction; cell cycle; ATPases associated with diverse cellular activities (AAA); protein complex; *Escherichia coli*; nucleic acid; flow cytometry

---

ABSTRACT

Timely initiation of replication in *Escherichia coli* requires functional regulation of the replication initiator, ATP-DnaA. The cellular level of ATP-DnaA increases just before initiation, after which its level decreases through hydrolysis of DnaA-bound ATP, yielding initiation-inactive ADP-DnaA. Previously, we reported a novel DnaA-ATP hydrolysis system involving the chromosomal locus *datA*, and named it *datA*-dependent DnaA-ATP hydrolysis (DDAH). The *datA* locus contains a binding site for a nucleoid-associating factor IHF and a cluster of three known DnaA-binding sites, which are important for DDAH. However, the mechanisms underlying the formation and regulation of the *datA*–IHF–DnaA complex remain unclear. We now demonstrate that a novel DnaA box within *datA* is essential for ATP-DnaA complex formation and DnaA-ATP hydrolysis. Specific DnaA residues, which are important for interaction with bound ATP and for head-to-tail inter-DnaA interaction, were also required for ATP-DnaA-specific oligomer formation on *datA*. Furthermore, we show that negative DNA supercoiling of *datA* stabilizes ATP-DnaA oligomers, and stimulates *datA*–IHF interaction and DnaA-ATP hydrolysis. Relaxation of DNA supercoiling by addition of novobiocin, a DNA gyrase inhibitor, inhibits *datA* function in cells. On the basis of these results, we propose a mechanistic model of *datA*–IHF–DnaA complex formation and DNA supercoiling-dependent regulation for DDAH.

In *Escherichia coli*, the ATP-bound DnaA protein (ATP-DnaA) has an essential role in assembly of initiation complexes on the chromosomal replication origin *oriC* (1–5). *oriC*

consists of an AT-rich duplex-unwinding element and a DnaA-oligomerization region that contains two subregions with oppositely-oriented clusters of 9 bp DnaA-binding sites (DnaA boxes) (Fig. 1*A*). DnaA boxes R1 and R4 at the outer edges of the DnaA-oligomerization region are oriented oppositely and have the highest affinities for DnaA of the sequences in this region. Cooperative binding of ATP-DnaA molecules to lower affinity sites in each subregion of *oriC* results in formation of the left-half and right-half DnaA subcomplexes (6–8). The left-half subcomplex binds to the region of *oriC* that contains the duplex-unwinding element, and executes unwinding of DNA within the element (6, 9). IHF, a nucleoid-associated protein (NAP), binds to a specific IHF-binding site (IBS; Fig. 1*A*) within the left-half subregion of *oriC*, and bends DNA sharply (~180°), enhancing ATP-DnaA binding and duplex unwinding (9, 10). The DnaA subcomplexes interact also with a pair of DnaB helicases for loading of those to the single-stranded DNA (9, 11, 12).

DnaA consists of four domains (3). The N-terminal domain I has a DnaB-binding site (12). Domain II is a flexible linker (12). Domain III is the AAA+ domain that has motifs for binding and hydrolysis of ATP (Walker A and B and Sensor I and II), and for interaction between DnaA protomers (arginine-finger, Box VII, AID-1, and AID-2) (Fig. 1*B*) (6, 13–16). DnaA arginine-finger Arg285 has a key role in ATP-dependent head-to-tail interaction between DnaA protomers, which activates the formation of subcomplexes on *oriC* (7, 13). DnaA Box VII Arg281 residue stabilizes the interaction (16). AID-1 Arg227 and AID-2 Leu290 residues stimulate protomer interactions in the left-half DnaA subcomplex (6). The C-terminal DnaA domain IV contains the helix-tern-helix motif bearing DnaA box-binding activity (17).

Initiation of replication from *oriC*, and especially duplex unwinding, is regulated by negative DNA supercoiling (18), which is modulated by the actions of DNA topoisomerases such as DNA gyrase, and by binding of NAPs. DNA supercoiling is involved in regulation of multiple cellular processes, including DNA replication, transcription, recombination, and nucleoid compaction (19–21). The supercoiling state of chromosomal DNA is altered dynamically according to the growth phase and extracellular stresses such as osmotic shock, heat, pH, and antibiotics, to sustain cell growth (22–25). For example, in the osmotic transcriptional response in *E. coli*, DNA supercoiling regulates the association of RNA polymerase on DNA, and expression of osmotic-response genes (23, 26). In *Helicobacter pylori*, DNA supercoiling affects the binding mode of the cognate DnaA and *oriC* (27). However, the importance of supercoiling-dependent regulation for cellular DnaA activity remains unclear.

The cell cycle-coordinated initiation of chromosomal replication is sustained by multiple regulatory systems that affect cellular DnaA activity (1, 4, 28). After ATP-DnaA induces replication initiation, DnaA-ATP is hydrolyzed by the complex of the AAA+ domain-containing Hda protein and the DNA-loaded β-clamp subunit of the DNA polymerase III holoenzyme, yielding initiation-inactive ADP-DnaA (1, 29–31). This replication-coupled feedback system is called regulatory inactivation of DnaA (RIDA). Defects in RIDA result in overinitiation and the

inhibition of cell growth (15, 32).

Previously, we demonstrated that a specific chromosomal locus (*datA*) promotes DnaA-ATP hydrolysis by a mechanism that we named *datA*-dependent DnaA-ATP hydrolysis (DDAH) (33). The *datA* locus (991 bp) includes a 262 bp region containing two known DnaA-box sequences (DnaA boxes 2 and 3) and an IBS, which is essential for repression of untimely initiation (Fig. 1*A*) (25–28). DNA-footprinting experiments suggest the presence of two further sites within the 262 bp *datA* region that bind DnaA (herein described as DnaA boxes 6 and 7) (Fig. 2*A*) (35). However, the roles of these boxes remain to be explored.

DnaA sensor II-motif Arg334 residue has a key role in DnaA-ATP hydrolysis in RIDA and DDAH (Fig. 1*B*) (15). DnaA arginine-finger Arg285 and Box VII Arg281 are also required for DDAH, but not for RIDA (Fig. 1*B*) (13, 33). IHF temporarily binds to *datA* at the post-initiation stage and ensures once-per-cell-cycle initiation. However, the underlying mechanism of inter-DnaA interactions in DDAH and its regulation have not yet been determined.

We demonstrated that *datA* DnaA box 7, but not box 6, has an essential role in DDAH, and that DnaA box 7 stimulates cooperative binding of ATP-DnaA on *datA*. Second, we showed that the DnaA AID-2 motif, but not AID-1, is required for DDAH. Third, we found that the DnaA arginine-finger, Box VII, and AID-2 motifs are required for ATP-DnaA-specific oligomer formation on *datA*. Fourth, we identified that negative DNA supercoiling stimulates DDAH. DNA supercoiling has little effect on the overall structure of *datA*-DnaA complexes, but stabilizes ATP-DnaA oligomer formation and stimulates binding of IHF to *datA*. Consistent with these *in vitro* findings, activity of *datA in vivo* was impaired in the presence of novobiocin, an inhibitor of DNA gyrase. From these results, we propose a model of the mechanism of DDAH and its regulation by DNA supercoiling.

RESULTS

Cooperative DnaA binding to datA DnaA boxes 2 and 7 is essential for DDAH - We previously reconstituted the DDAH system *in vitro* with ATP-DnaA, IHF, and a DNA fragment containing a 991 bp *datA* sequence, and found that DnaA boxes 2 and 3 and IBS were required for DDAH activity (33). Data from previous *in vivo* analyses are consistent with these *in vitro* results (35, 36). A *datA* region between DnaA boxes 1 and 2 might contain two additional DnaA boxes (boxes 6 and 7) with moderate homology with the consensus sequence (Fig. 2*A*) (35). To determine the involvement of DnaA boxes 6 and 7 in DDAH, we generated constructs with transversion mutations at these sites in bases that are identical to the DnaA-box consensus sequence. Inclusion of these mutant sequences in the reconstituted *in vitro* DDAH system indicated that DnaA box 7 was required for DDAH, whereas DnaA box 6 was dispensable (Fig. 2*B*).

To determine whether formation of DnaA oligomers at *datA* is inhibited by mutation of DnaA box 7, EMSA (electrophoretic mobility shift assay) was performed with the minimal *datA* region that is competent for DDAH (*datA* del5; Fig. 2*C*), in the presence of IHF and either ATP-DnaA or ADP-DnaA. ATP-DnaA formed large complexes (≥C5 with at least five DnaA molecules per substrate molecule of *datA* del5

when the input molar ratio was 13–20 DnaA per *datA* (Fig. 2, *D* and *E*). By contrast, ADP-DnaA mainly formed smaller complexes (C1–C4) with one to four DnaA molecules per substrate, consistent with previous results (33). Both ATP-DnaA and ADP-DnaA formed mainly smaller complexes on *datA* del5 with a DnaA box 7 mutation (subDnaAbox7; Fig. 2, *D* and *F*).

EMSA was also conducted with short dsDNA fragment (*datA* 672 fragment; 43 bp) containing DnaA boxes 6, 7, and 2. Mutation of individual DnaA-box sequences demonstrated that binding of DnaA to box 7 was dependent on box 2 (Fig. 2*G*). These results indicate that cooperative DnaA binding involving box 7 and box 2, but not box 6, is essential for formation of ATP-DnaA oligomers that are required to activate DDAH.

Inter-DnaA interaction motifs are required for ATP-DnaA-specific oligomerization on datA

Previously, we revealed that DnaA AAA+ motifs, arginine-finger Arg285 and Box VII Arg281 (Fig. 1*B*), are required for DDAH (33). Here, we assessed the DDAH requirements for inter-DnaA interaction motifs AID-1 Arg227 and AID-2 Leu290. These residues are required for initiation of chromosomal replication and are thought to be important in specific inter-DnaA interactions in initiation complexes (6). In addition, the AID motifs are important in DnaA functions in *DARS2* (DnaA reactivating sequence 2), which is a specific DnaA-binding locus on the chromosome and stimulates ADP-to-ATP exchange of DnaA, yielding ATP-DnaA in a timely manner (4, 37). AID-2 Leu290 is essential for DnaA oligomerization on *DARS2* and for DnaA-ADP dissociation by *DARS2*, and AID-1 Arg227 plays a stimulatory role in DnaA-ADP dissociation by *DARS2* (37).

In the reconstituted DDAH assay, DnaA L290A was defective for DDAH activity, whereas DnaA R227A showed only a slight inhibition of DDAH activity (Fig. 3*A*). To address the requirement for AID-2 Leu290 in ATP-DnaA-specific oligomerization on *datA*, we performed EMSA with a DnaA L290A mutant protein (Fig. 3, *B–D*). Unlike wild-type (WT) ADP-DnaA, ADP-DnaA L290A efficiently formed large oligomers on *datA* del5 (Fig. 3, *B–D*). These results suggest that inter-DnaA interaction via AID-2 destabilizes ADP-DnaA oligomers on *datA*, which stimulates successive interactions of ATP-DnaA molecules on *datA*, elevating the catalytic reaction rate of DDAH. Another possibility is that DnaA L290A forms oligomers on *datA* via irregular inter-DnaA contacts independently of the bound nucleotides.

The DnaA arginine-finger Arg285 and Box VII Arg281 have important roles in the inter-DnaA interactions within *oriC* initiation complexes, and are required for DDAH (33). EMSA was performed using *datA* and DnaA R285A and R281A mutant proteins (Fig. 3, *E–J*). DnaA R285A was defective in formation of large ATP-DnaA oligomers on *datA* del5 (Fig. 3, *E–G*), indicating that inter-ATP-DnaA interaction via Arg285 is required for specific DnaA oligomerization, which is a prerequisite for DDAH. By contrast, DnaA R281A showed moderate ATP-DnaA-specific oligomerization on *datA* (Fig. 3, *H–J*).

datA DnaA box 7 is required to repress untimely initiation in vivo - To investigate the *in vivo* function of *datA* DnaA box 7, flow cytometry analysis was performed on MG1655 cells with plasmids containing *datA* (pKX40) or

its mutant derivatives, which were cultivated at 37°C in LB medium (Fig. 4*A*). To determine the number of *oriC* copies, growing cells were incubated in the presence of rifampicin and cephalexin (inhibitors of replication initiation and cell division, respectively) until chromosomal replication was complete. The number of chromosomes per cell determined by flow cytometry then corresponds to the number of *oriC* copies per cell at the time of addition of the antibiotics (37–39). In rapidly growing cells, depending on growth conditions, a single cell contains two, four, or four sister *oriC* copies before replication initiation, and initiation occurs simultaneously on each *oriC* copy while the previous round of replication is ongoing, resulting in four, eight, or sixteen copies of *oriC* in a cell (38).

The results of flow cytometry showed that, whereas MG1655 cells with the pACYC177 plasmid (which does not contain *datA*) had eight or sixteen replication origins per cell, those with pKX40 contained four or eight origins, and some cells had six origins, as a result of asynchronous initiation (Fig. 4*A*). The asynchronous index (Ai), which evaluates the level of improper timing of initiation (38, 40–42), was increased in cells with pKX40 compared with pACYC177 (46% versus 4.8%). In cells with pKX40, the origin number to mean cell mass (ori/mass), an indicator of initiation activity, was reduced to 0.67 relative to the reference value of 1.0 in cells with pACYC177. These results were consistent with those of previous studies (43, 44), and indicated that oversupply of *datA* moderately inhibited initiation. In addition, introduction of pKX40 caused moderate reduction in cell growth relative to pACYC177 (doubling time (Td) 38 min versus 26 min), along with delay in the timing of cell division (cell mass with pKX40 1.3 × cell mass with pACYC177). By contrast, initiation parameters and growth rates were not substantially affected by oversupply of the *datA* substitution mutants subDnaAbox7 (pHT28) or subDnaAbox2 (pKX41), whereas subDnaAbox6 (pKX120) inhibited initiations and cell growth like the WT *datA* (pKX40) (Fig. 4*A*), all of which is consistent with our *in vitro* data (Fig. 2*B*).

ori/mass ratios and Ai were also analyzed in cells with chromosomal *datA* mutations (Fig. 4, *B* and *C*). In Δ*datA* cells, synchronous initiation was severely inhibited (Ai = 90%) and the number of *oriC* copies per cell increased compared with WT cells, but initiation frequency and cell growth were hardly affected (Fig. 4*B*), as reported previously (34, 35, 45). Cells with *datA* mutations had growth rates comparable to those of WT or Δ*datA* cells (Fig. 4, *B* and *C*). In LB medium, chromosomal *datA* subDnaAbox7 or subDnaAbox2 mutants exhibited severe asynchronous initiation (Ai = 114% or 127%, respectively), whereas a subDnaAbox6 mutant did not (Ai = 9.2%; Fig. 4*B*), further indicating that DnaA box 7 is essential for *datA* function *in vivo*. Similar results were obtained in cells cultivated in supplemented M9 medium (Fig. 4*C*), except for an unexpected increase in cell mass in the presence of *datA* mutations. The delay in cell division implies that DnaA boxes 6, 7, or 2 might have supportive roles in the regulation of cell division by *datA*, as suggested previously (46). Also, in *datA* subDnaAbox6 mutant cells, initiation frequency was slightly decreased (ori/mass = 0.83 or 0.85 in LB or supplemented M9 medium, respectively) compared with that

in WT cells, suggesting the possibility that *datA* DnaA box 6 might repressively regulate DDAH *in vivo* at a limited level.

Negative DNA supercoiling promotes DDAH efficiency - To assess whether DNA supercoiling affects DDAH activity, ATP-DnaA and IHF were incubated with a supercoiled or PstI-digested linear form of the *datA*-containing plasmid pKX40 (Fig. 5*A*). ATP-DnaA molecules were efficiently converted into ADP-DnaA at 30°C for 10 min in buffer containing 100 mM NaCl and either the supercoiled or linear form of pKX40 (Fig. 5, *B* and *C*), consistent with previous results in buffer containing 100 mM potassium glutamate (33). The parental vector, pACYC177, did not substantially show DDAH activity: only a slight activity would be caused by feeble DnaA-intrinsic ATPase (47). To address a question of whether DNA supercoiling stabilizes nucleoprotein complexes on *datA*, we examined resistance of DDAH activity against higher salt concentrations (i.e., 150 or 200 mM NaCl). Notably, whereas DDAH activity of the supercoiled form of pKX40 was resistant to 150 mM and 200 mM NaCl, that of the linear form was moderately inhibited at 150 mM NaCl and the activity was further aggravated at 200 mM (Fig. 5, *B* and *C*).

In the presence of 150 mM NaCl, DDAH activities of the supercoiled and linear forms were further analyzed. Both DNA-titration and time-course experiments indicated that DDAH catalyzed by *datA* in a supercoiled form was more efficient than that by *datA* in a linear form (Fig. 5, *D* and *E*). One molecule of supercoiled *datA* promoted hydrolysis of 3.3 ATP-DnaA molecules per min, whereas hydrolysis was only 1.9 ATP-DnaA molecules per min with linear *datA*.

DNA supercoiling slightly altered the requirement for IHF in DDAH. The maximal reaction rate was achieved with 0.15 pmol IHF on supercoiled *datA*, but 0.3 pmol IHF on linear *datA* (Fig. 5*F*), implying that DNA supercoiling might stimulate formation of *datA*–IHF complexes. The physiological ionic strength is 100–150 mM, suggesting that DNA supercoiling can stimulate DDAH activity under certain physiological conditions.

Structural requirements of supercoiled datA in DDAH - Our previous results with linear *datA* fragments indicated that DnaA box 2–3 and IBS are essential for DDAH, whereas DnaA box 4 is stimulatory (33). To identify the specific requirements of supercoiled *datA* in DDAH, the activities of various deletion derivatives of the *datA* WT fragment were analyzed in the presence of 150 mM NaCl (Fig. 6*A*). As with linear *datA* (33), full DDAH activity was sustained by the supercoiled form of *datA* del5 (pHT20), which contains DnaA boxes 6, 7, 2–4, and IBS (Fig. 6*A*). Furthermore, the supercoiled form of *datA* del6 (pHT21), which lacks DnaA box 4, also displayed full DDAH activity. As the DDAH activity of linear *datA* del6 DNA was moderately inhibited compared with that of the del5 DNA (33), these data suggest the possibility that DNA supercoiling stimulates DnaA oligomerization, promoting efficient DnaA-ATP hydrolysis. By contrast, the supercoiled forms of the *datA* del7 and del8 fragments (pHT22 and pHT23), which lack crucial DnaA box 3 and boxes 2 and 7, respectively, were largely inactive (Fig. 6*A*), consistent with our previous results with linear *datA* (33).

A similar assay was used to analyze

substitution mutants of DnaA boxes and the IBS (Fig. 6*B*). These substitution mutants are largely inactive for DnaA and IHF binding, respectively (35, 36). Results from the DDAH assay indicated that DnaA boxes 7, 2, and 3, and IBS, but not DnaA boxes 4 or 6, were essential for DDAH even in the supercoiled form (Fig. 6*B*), supporting the results with the deletion derivatives (Fig. 6*A*). In particular, the supercoiled form of *datA* subDnaAbox4 DNA sustained full DDAH activity (Fig. 6*B*); consistently, box 4 has previously been shown to be dispensable for regulation of initiation *in vivo* (36).

Modes of inter-DnaA interactions in DDAH with a supercoiled form of datA - To further analyze the mechanism of DDAH promoted by supercoiled *datA*, DDAH activities were analyzed using a series of DnaA mutants and pKX40 or pACYC177 vector (Fig. 7). The DnaA L290A mutant was slightly active for DDAH with a supercoiled *datA* form, and was substantially inactive with a linear form (Fig. 7, *A* and *B*). By contrast, the DnaA R227A mutant fully sustained DDAH activity with a supercoiled *datA* form, and was slightly impaired with a linear form (Fig. 7, *A* and *B*). These results are consistent with the data shown in Fig. 3*A–D* and with the idea that assembly of ATP-DnaA molecules on *datA* occurs in a partly different manner to that on *oriC* and *DARS2* (6, 33), and that supercoiling assists in functional inter-DnaA interaction on *datA*.

Consistent with the results of a previous study with linear *datA* (33), the DnaA R281A mutant induced very low DDAH activity with both the supercoiled and linear forms of *datA* (Fig. 7, *C* and *D*), suggesting an essential role for Box VII Arg281-dependent inter-DnaA interactions in DDAH. By contrast, DnaA R285A showed moderately reduced activity with supercoiled *datA*, and very low activity with the linear form (Fig. 7, *C* and *D*). These results suggest that the arginine-finger Arg285-dependent inter-DnaA interactions are less important for DDAH with supercoiled *datA* than with linear *datA*.

In DnaA-ATP hydrolysis by RIDA and DDAH with the linear *datA* form, DnaA AAA+ sensor II Arg334 is essential (15, 33). This residue is proposed to interact with the phosphate moiety of ATP bound to DnaA, promoting hydrolysis of ATP (15, 48, 49). DnaA R334A was substantially inactive in DDAH even with the supercoiled *datA* form (Fig. 7, *E* and *F*), indicating the importance of Arg334 in DDAH.

DNA supercoiling stabilizes DnaA oligomerization and IHF binding on datA - To assess whether DNA supercoiling stabilizes DnaA oligomerization on *datA*, a BglII-protection assay was performed (Fig. 8, *A–C*). The BglII recognition sequence, AGATCT, was introduced into the native CGATCA sequence in the region for ATP-DnaA oligomerization of pKX40 (33), yielding pKX133 (Fig. 8*A*). The introduced sequence had only two bases substitution and resided in the intervening region between IBS and DnaA box 3. In the protection assay, ATP-DnaA was incubated on ice with pKX133 in 100 mM NaCl buffer in the absence of IHF, followed by incubation at 30°C with BglII. The results showed that BglII digestion of pKX133 was inhibited in a DnaA dose-dependent manner regardless of the linear or supercoiled form of *datA* (Fig. 8*B*), which indicates that extended DnaA oligomers are formed in the region and

protect the DNA from BglII, consistent with the EMSA data (Fig. 3). By contrast, when similar experiments were performed in 150 mM NaCl buffer, protection of the supercoiled form was preserved, but protection of the linear form was considerably decreased (Fig. 8*C*). These results are consistent with the idea that DNA supercoiling stabilizes the extended DnaA oligomers, and also with the changes in DDAH activities shown in Fig. 5B-E.

A protection analysis was also performed using EcoRV to assess whether DNA supercoiling affects IHF binding to *datA* (Fig. 8, *D–G*). IHF binding to double-stranded oligonucleotides containing a *datA* IBS was not greatly affected by introduction of the EcoRV site within the IBS (Fig. 8*E*). An EcoRV-protection assay with pHT25, a pKX40 derivative bearing the EcoRV site, indicated that IHF protected a supercoiled IBS region from EcoRV more effectively than a linear IBS in 100 or 150 mM NaCl buffer (Fig. 8, *F* and *G*). These results suggest that DNA supercoiling stabilizes IHF binding to *datA* independently of salt concentration.

Modulation of DNA supercoiling by novobiocin decreases datA function in vivo

To investigate the *in vivo* role of DNA supercoiling in stimulation of DDAH, we assessed whether relaxation of negative DNA supercoiling suppresses growth inhibition caused by oversupply of *datA*. Consistent with previous results (44), introduction of pKX88 (pBR322-*datA*) severely retarded colony formation of MG1655 (WT) cells grown at 37°C in NaCl-depleted LB medium (Fig. 9*A*). By contrast, KMG-5 (Δ*ihfA*) cells bearing pKX88 formed colonies at a level similar to that of those bearing the parental vector pBR322. When similar experiments were performed in the presence of a moderate concentration (15 μg/ml) of novobiocin, an antibiotic that inhibits the function of DNA gyrase and relaxes DNA supercoiling (Fig. 9*A*) (50), MG1655 cells bearing pKX88 had similar colony-forming ability to those bearing pBR322, or to KMG-5 (Δ*ihfA*) cells. Addition of novobiocin suppressed growth inhibition caused by oversupply of *datA in vivo*.

Flow cytometry was performed to examine the replication-initiation timing of cells harboring pKX88 (pBR322-*datA*), growing at 37°C in NaCl-depleted LB medium including novobiocin (Fig. 9, *B* and *C*). The results showed that, whereas MG1655 cells bearing pBR322 contained four or eight origins, those bearing pKX88 contained one, two, or four origins and some cells experienced asynchronous initiations (Fig. 9*B*). In cells bearing pKX88, ori/mass was reduced to 0.73 relative to a ratio of 1.0 in cells bearing pBR322. These results are consistent with those shown in Fig. 4*A*, and with previous studies (44), and indicate that oversupply of *datA* severely inhibits initiation. In KMG-5 (Δ*ihfA*) cells bearing pBR322, regulation of initiation was disrupted, causing untimely initiations, consistent with previous reports (37, 51). Unexpectedly, introduction of pKX88 inhibited initiation in KMG-5 cells (ori/mass = 0.74), probably because of DnaA titration on *datA* in an IHF-independent manner. Addition of novobiocin (15 μg/ml) slightly inhibited initiation in MG1655 cells bearing pBR322. Notably, in the presence of novobiocin, the *oriC* number per cell in MG1655 cells bearing pKX88 was increased compared to that in the absence of novobiocin, and ori/mass in those

cells was only reduced to 0.91 relative to a ratio of 1.0 in MG1655 cells bearing pBR322 (Fig. 9, *B* and *C*). By contrast, addition of novobiocin had little effect on initiation in KMG-5 cells bearing pKX88 (ori/mass = 0.78), supporting the idea that DNA supercoiling might specifically stimulate DDAH (rather than initiation *per se*).

To assess whether relaxation of DNA supercoiling occurred in cells cultivated in NaCl-depleted LB medium containing novobiocin, the structures of plasmid topoisomers and the copy number of plasmids were examined. To analyze topoisomers, plasmids were subjected to electrophoresis in agarose gels containing chloroquine, which induces positive DNA supercoiling into plasmids. Consistent with a previous report (52), addition of 15 μg/ml novobiocin relaxed negative DNA supercoiling of pBR322 (Fig. 9*D*). Plasmid copy numbers were analyzed by quantitative PCR. As a control for chromosome number, we quantified the signal intensity of the *ter* locus, a termination site of DNA replication (53). Quantification of relative plasmid signal by amplifying the *tet* gene of pBR322 revealed that addition of novobiocin had little effect on plasmid copy numbers (Fig. 9*E*). Previous transcriptome analysis revealed that relaxation of DNA supercoiling by drug addition had little effect on the expression of IHF (54), implying that suppression of growth inhibition by oversupply of *datA* was caused by reduction of DNA supercoiling, resulting in inhibition of plasmid *datA*-derived DDAH.

DISCUSSION

This study revealed the functional structure of ATP-DnaA oligomers associated with *datA* and IHF, and demonstrated the fundamental role of negative DNA supercoiling in the regulation of DDAH. Our results identified that *datA* DnaA box 7, as well as DnaA AID-2 Leu290, were required for DDAH (Fig. 2*B*, 3*A*, 4, 6*B*, 7, *A* and *B*, and summarized in 10*A*). Binding of ATP-DnaA on *datA* DnaA box 7 is probably assisted by head-to-tail inter-DnaA interaction with DnaA bound to the neighboring DnaA box 2, which has the same orientation as box 7 (Fig. 2*A*) (7). Consistently, the DnaA arginine-finger Arg285 and Box VII Arg281, which are required for formation and stabilization, respectively, of ATP-DnaA-specific oligomers on *oriC* (13, 16, 33), were also essential for DDAH promoted by linear *datA* (Fig. 3*A* and 10*A*). These results are supported also by the 3 bp interval between boxes 2 and 7 in *datA*, which is preferable in interaction between DnaA molecules bound to adjacent boxes (Fig. 2*A*) (8). Furthermore, formation of ATP-DnaA oligomers on *datA* depends on the arginine-finger motif, but not on AID-2 (Fig. 3, *B–G*). Similar mechanisms might be also involved in inter-DnaA interaction for DnaA bound to the right-half *oriC* subregion (Fig. 10*A*) (6, 13). In the left-half *oriC* subregion, a functional ATP-DnaA oligomer is sustained by the arginine-finger-, and AID-1&2-dependent tight cooperative binding between two DnaA boxes with a 2 bp interval, which is required for DUE unwinding (Fig. 10*A*) (6). These observations suggest the possibility that ATP-DnaA oligomers formed on DnaA boxes 2 and 7 with a 3 bp interval might engage a relatively loose inter-DnaA contact, triggering interaction between DnaA sensor II Arg334 and ATP and activating DnaA-ATP hydrolysis specifically on *datA*. Our observation that

oligomers of ADP-bound DnaA L290A mutant were somehow stabilized on *datA* suggests a possibility that DnaA AID-2 Leu290 participates in a process of dissociation of ADP-DnaA from *datA* in DDAH reactions (Fig. 3, *B–D*). Different requirements for specific DnaA motifs in functions at *oriC* (DUE unwinding), *datA*, and *DARS*s are consistent with differentiation in structure-function relationship of DnaA complexes on those sites (Fig. 10*A*).

Our results showed that negative DNA supercoiling increases the efficiency of the DDAH reaction, and stabilizes it against conditions of 150–200 mM NaCl (Fig. 5, *B* and *C*). Mechanistic analysis revealed that DNA supercoiling assisted DnaA oligomerization as well as IHF binding on *datA* in 150–200 mM NaCl, which is consistent with the results of previous studies of IHF binding to $ilvP_G$ promoter and IS1 (55, 56). The necessary elements within *datA* and DnaA for DDAH with supercoiled *datA* were almost the same as for DDAH with linear *datA*, except that, with supercoiled *datA*, the DnaA arginine-finger was stimulatory, but not essential (Fig. 6 and 7). DNA supercoiling stabilized oligomerization of ATP-DnaA (Fig. 8, *A–C*). These results suggest that DnaA AID-2 Leu290 and Box VII Arg281 are more important for ATP-DnaA-specific oligomerization and inter-DnaA interactions formed in supercoiled *datA* than the interaction between the arginine-finger and ATP.

On the basis of our results, we propose a mechanistic model of DDAH (Fig. 10*B*). In the first step of this model, ATP-DnaA cooperatively binds on the left-hand subregion of *datA* that includes DnaA boxes 2 and 7, and on the right-hand subregion that includes DnaA box 3. The two subregion oligomers might interact with each other in a head-to-tail manner, with the aid of DNA bending by IHF. The DnaA arginine-finger is also essential for the cooperative ATP-DnaA oligomerization on linear *datA* (Fig. 3, *E–G*), and DnaA Box VII Arg281 supports tight inter-DnaA interactions in complexes involving *datA* and IHF. The arginine-finger side of DnaA orients toward the 5' end of the DnaA-box consensus sequence, and the ATP-bound side of DnaA has the opposite orientation (7). Negative DNA supercoiling stabilizes ATP-DnaA oligomers against dissociation caused by high salt concentrations, and promotes IHF binding (Fig. 8), probably via stabilization of the DNA loop. DnaA would also bind to DnaA boxes 4 and 6, although their roles in DDAH are minimal. Then, in this complex, DnaA-ATP hydrolysis by DnaA Sensor II Arg334 is activated by the two possible mechanisms (Fig. 10*B*); in Model 1, loose interaction of ATP-DnaA protomers bound on DnaA boxes 7 and 2 might induce conformational change of nucleotide pocket, following interaction with box 3-bound ATP-DnaA to activate DnaA-ATP hydrolysis of box 7-bound DnaA. Sharp DNA bending by IHF might stimulate the interaction between ATP-DnaA protomers bound to DnaA boxes 2 and 3. In another mechanism (Model 2), DNA bending by IHF induces functional interaction between the protomers bound to DnaA boxes 2 and 3, thereby activating DnaA-ATP hydrolysis of ATP-DnaA oligomer on the left-hand subregion (Fig. 10*B*). In either of the cases, DnaA Box VII Arg281 might modulate the structure of ATP-DnaA oligomers on the complexes. Finally, the resultant ADP-DnaA might be destabilized and dissociated from *datA*

via the action of DnaA AID-2 Leu290. The present data that we have can not allow for distinction of these possible mechanisms. Those could be further elucidated using a chimeric DnaA molecule which can bind to a different DnaA box sequence (7); we consider that this might be an important future study.

Our observations of DNA supercoiling-dependent stimulation of IHF binding (Fig. 8, *D–G*) are consistent with the possibility that cell cycle-coordinated IHF binding to *datA* and *DARS2* is regulated by changes in DNA supercoiling. Our previous finding that addition of rifampicin inhibits timely dissociation of IHF from *datA* (33) is consistent with the current observations; rifampicin is an antibiotic drug that dissociates running RNA polymerases from the chromosome and reduces DNA supercoiling (57). Studies have also demonstrated that transcription of *yjeV* (*ORF2.1*) and *queG* (*ORF43*) genes can pass through the *datA* essential region (43), and thus alteration of *datA* DNA supercoiling by transcription is a potential mechanism for regulation of timely IHF binding.

Unlike DnaA from *E. coli* and *Bacillus subtilis*, DnaA from *Helicobacter pylori* efficiently assembles on the supercoiled form of the cognate *oriC* rather than the relaxed form (27, 58, 59). Similarly, in *Drosophila melanogaster*, supercoiled DNA has 30-fold higher affinity than linear DNA for the Origin recognition complex (60). As such, supercoiling of DNA might be of general importance for regulation of initiator–DNA binding. In many bacterial species including *B. subtilis* and *Streptomyces coelicolor*, DnaA box cluster-dependent repression systems for replication initiation are suggested to have roles similar to those of DDAH (61, 62), and supercoiling-mediated regulation could be important for DnaA assembly on the DnaA-box clusters underlying these systems.

Like IHF, HMG1 protein, which belongs to the high mobility group family, a eukaryotic counterpart of NAPs, as well as MC1 protein, which is an archaebacterial histone-like protein, have higher affinity for supercoiled DNA than for relaxed DNA (63, 64). DNA supercoiling-dependent regulation of the binding of chromosome-structuring proteins could be conserved widely in prokaryotic and eukaryotic species.

EXPERIMENTAL PROCEDURES

Proteins, DNA, and E. coli *strains* - DnaA proteins and IHF were overexpressed and purified from *E. coli* cells, as previously described (9, 33).

The following plasmids were described previously (33): pKX62 (*datA*ΔIBS), pKX48 (subDnaAbox1), pKX41 (subDnaAbox2), pKX43 (subDnaAbox3), pKX47 (subDnaAbox4), pKX49 (subDnaAbox5), and pKX42 (subIBS). A WT *datA* fragment (991 bp) was cloned into pACYC177 plasmid to yield pKX40, as described (33). pKX40 derivatives containing *datA*-sequence substitutions were constructed by inside-out PCR from pKX40 with the following primers: subL1-U and subL1-L for pKX120 (subDnaAbox6), tnk126datAlow-F and tnk128datAlow-R for pHT28 (subDnaAbox7), 40BglII-U and 40BglII-L for pKX133 (IBS-DnaA box 3 linker$_{BglII}$), and tnk124IBSEcoRV-F and tnk125IBSEcoRV-R for pHT25 (IBS$_{EcoRV}$). The *datA* fragment (991 bp) and its derivatives,

which were used in Fig. 2*B*, were amplified from pKX40, pKX48 (subDnaAbox1), pKX120 (subDnaAbox6), pHT28 (subDnaAbox7), and pKX41 (subDnaAbox2) with primers datA-1 and datA-2 (Table 1). The *datA* minimal region for DDAH (del5) and its derivatives, which were used in EMSA, were amplified from pKX40, pKX62 (ΔIBS), and pHT25 (IBS_{EcoRV}) with primers datA-3 and datA-6, and from pKX40 with primers datA-3 and datA6subDnaAbox7 for subDnaAbox7 (Table 1). Derivatives of *datA* 672 fragments that were used for EMSA (Fig. 2*F*) are shown in Table 1 and these oligonucleotides were annealed at room temperature overnight (672WT-U and 672WT-L for WT sequence, sub672-U and sub672-L for subDnaAbox6, 6sub72-U and 6sub72-L for subDnaAbox7, 67sub2-U and 67sub2-L for subDnaAbox2). For construction of chromosomal *datA* mutants, pTH5 plasmid was digested with EcoRI, and the resultant *frt-kan* gene (the kanamycin-resistance gene flanked by FRT site-specific recombination sequences) was cloned into the EcoRI sites of an inside-out PCR fragment amplified from pKX40 with primers datAEcoRI-U and datAEcoRI-L, resulting in pKX40kan. Truncated *datA* derivatives were amplified by PCR from pKX40 or pKX62 (ΔIBS) with the following primers: tnk121datA-1 and tnk116datA-3 for del2, tnk122datA-2 and tnk117datA-6 for del3, tnk116datA-3 and tnk117datA-6 for del5 and del5DIBS, tnk117datA-6 and tnk120datA-10 for del6, tnk117datA-6 and tnk119datA-9 for del7, and tnk116datA-3 and tnk118datA-7 for del8 (see Table 1 for each sequence). These fragments were inserted into the BamHI and HindIII sites of pACYC177 to yield pHT17 (del2), pHT18 (del3), pHT20 (del5), pHT24 (del5ΔIBS), pHT21 (del6), pHT22 (del7), and pHT23 (del8). A *datA* WT fragment (991 bp) was also cloned into the NruI site of pBR322 plasmid to yield pKX88.

All *E. coli* strains used in this study are listed in Table 2. Δ*datA*::*kan* mutation, derived from RSD448 cells, was introduced into MG1655 cells using P1 transduction, yielding strain MIT128. Chromosomal *datA* mutants with DnaA-box substitutions were introduced into MG1655 cells harboring pKD46 (65); DNA fragments carrying the *datA* mutation and *frt-kan* gene were amplified from pKX40kan with the following primers: ChdatAKn and datA-2 for *datA* WT-*frt-kan*, ChdatAKn and ChdatAsub6 for subDnaAbox6-*frt-kan*, ChdatAKn and ChdatAsub7 for subDnaAbox7-*frt-kan*, ChdatAKn and ChdatAsub2 for subDnaAbox2-*frt-kan*. The resultant mutations (*datA* WT-*frt-kan*, subDnaAbox6-*frt-kan*, subDnaAbox7-*frt-kan*, and subDnaAbox2-*frt-kan*) were introduced into MG1655 cells by P1 transduction. *kan* gene sequences were removed by introduction of pCP20 plasmid (65), yielding strains SR01 (WT-*frt*), SR10 (subDnaAbox6-*frt*), SR30 (subDnaAbox7-*frt*), and SR06 (subDnaAbox2-*frt*), respectively.

M9 medium was supplemented with 0.2% glucose, 0.2% casamino acids, and 5 μg/ml thiamine; 100 μg/ml ampicillin was included, if required.

In vitro *reconstitution of DnaA-ATP hydrolysis* - This was performed basically as we previously described (33). For DDAH reconstitution using PCR fragments (Fig. 2*B* and 3*A*), [α-^{32}P]ATP-DnaA was prepared by incubation of nucleotide-free DnaA (apo-DnaA) on ice for 15 min in buffer containing 3 μM

[α-^{32}P]ATP. [α-^{32}P]ATP-DnaA (1 pmol) was then incubated with various amounts of DNA and/or proteins, as indicated, in 15 µl buffer H (20 mM Tris-HCl (pH 7.5), 10 mM magnesium acetate, 2 mM ATP, 8 mM dithiothreitol, and 100 µg/ml bovine serum albumin) including 100 mM NaCl instead of 100 mM potassium glutamate (33). DnaA-bound nucleotides were recovered on nitrocellulose filters, and were extracted by 1 M HCOOH and analyzed by thin-layer chromatography, as described previously (33).

For DDAH reconstitution with plasmid DNA (Fig. 5–7), [α-^{32}P]ATP-DnaA (1 pmol) was incubated with various amounts of DNA and/or proteins in 15 µl buffer H containing 150 mM NaCl. To construct linear forms of pKX40 derivatives and pACYC177, as a negative control, these plasmids were digested at a unique site with a restriction enzyme PstI, which specifically cleaves DNA at CTGCAG sequences.

EMSA - This was performed basically as we previously described (33). For the experiments shown in Fig. 2, *C–F* and Fig. 3, *B–J*, various amounts of ATP-DnaA or ADP-DnaA (WT or mutated) were incubated at 15°C for 5 min with the *datA* del5 DNA fragment (0.15 pmol) in the presence of 150 mM NaCl, 2 mM ATP or ADP, and 150 ng phage λDNA (as a nonspecific competitor), with or without 6 pmol IHF. DNA and DNA–protein complexes were analyzed by electrophoresis on 2% (w/v) agarose gels at 90 V for 120 min in Tris–borate buffer, with staining with ethidium bromide, as described previously (33).

For the experiments shown in Fig. 2*G*, indicated amounts of ATP-DnaA were incubated with *datA* 672 WT fragment (containing DnaA boxes 6, 7, and 2) or its derivatives at 30°C for 5 min in 10 µl buffer H including 150 mM NaCl and indicated amounts of DNA, followed by analysis with 7% polyacrylamide-gel electrophoresis (PAGE) at 90 V for 60 min in Tris–borate buffer, with staining by Gel-Star.

For the experiments shown in Fig. 8*E*, the indicated amounts of IHF were incubated with IBS DNA at 30°C for 5 min in 10 µl buffer H containing 150 mM NaCl and indicated amounts of DNA, followed by analysis with 5% PAGE at 90 V for 60 min in Tris–borate buffer.

Flow cytometry analysis - This was performed basically as we previously described (33). Cells were cultivated at 37°C in LB medium, supplemented M9 medium, or NaCl-depleted LB medium including 100 µg/ml ampicillin and 0 or 15 µg/ml novobiocin, until the A_{600} (absorbance at 600 nm) reached 0.1–0.2, followed by further incubation at 37°C for 4 h in the presence of 300 µg/ml rifampicin and 10 µg/ml cephalexin for run-out replication. The resultant cells were fixed, stained with SYTOX Green (Life Technologies), and analyzed with FACS Calibur (BD Biosciences), as described previously (37, 38).

BglII analysis of DnaA binding - The linear or supercoiled forms of plasmid pKX133 (10 fmol), which contains a *datA* sequence engineered with a BglII-recognition site between the IBS and DnaA box 3 ($datA_{BglII}$), were incubated on ice for 10 min with various amounts of DnaA in 10 µl buffer H including 100 or 150 mM NaCl and 1 mM ATP or ADP, followed by further incubation at 30°C for 45 min with BglII (New England Biolabs, 2.5 U). The reaction was terminated in SDS loading buffer, and DNA fragments were analyzed by

1% (w/v) agarose-gel electrophoresis.

EcoRV analysis of IHF binding - The linear or supercoiled forms of pHT25 (10 fmol), which contains a *datA* sequence engineered with an EcoRV recognition site flanking the IBS (*datA* IBS_{EcoRV}), were incubated at 30°C for 5 min with various amounts of IHF in 10 µl buffer H including 100 mM or 150 mM NaCl, followed by incubation at 30°C for 10 min with EcoRV (TOYOBO, 0.5 U). The resultant DNA fragments were analyzed as described above.

Chloroquine-gel electrophoresis and quantitative PCR - MG1655 cells containing pBR322 were cultivated at 37°C in 100 ml NaCl-depleted LB medium including 100 µg/ml ampicillin and 0 or 15 µg/ml novobiocin until A_{660} reached 0.2; then pBR322 was isolated. To assess the effects of novobiocin on DNA supercoiling, plasmid topoisomers were separated by 2.5 µg/ml chloroquine-0.65% (w/v) agarose-gel electrophoresis with Tris–borate–EDTA buffer. Approximately 50 ng plasmid DNA was loaded onto the gel using loading buffer (5% glycerol and 4 µg/ml bromophenol blue). Topoisomers were separated by electrophoresis at 20 V (1.5 V/cm) for 15 h, and stained by ethidium bromide.

For analysis of the plasmid copy number, cell suspensions were boiled, and the supernatants were collected by centrifugation. The levels of chromosomal *ter* locus and pBR322 *tet* gene in the supernatants were quantified by real-time qPCR using SYBR Premix Ex Taq II (Perfect Real Time) (Takara Bio) and the following primers: TER_2 and SUEterRev1 for *ter*, and SMT-7 and RTpBR322 for *tet* (see Table 1 for each sequence).

Conflict of interest: The authors declare that they have no conflict of interest of this article.

Author contributions: KK and TK designed the study. KK and HT performed most of the experiments, RS partly performed *in vitro* and *in vivo* experiments, and all authors analyzed and discussed about the data. KK and TK wrote the manuscript. All authors reviewed the manuscript and approved the final version.

REFERENCES

1. Katayama, T., Ozaki, S., Keyamura, K., and Fujimitsu, K. (2010) Regulation of the replication cycle: conserved and diverse regulatory systems for DnaA and *oriC*. *Nat. Rev. Microbiol.* **8**, 163–170
2. Leonard, A. C., and Grimwade, J. E. (2015) The orisome: Structure and function. *Front. Microbiol.* **6**, 1–13
3. Kaguni, J. M. (2011) Replication initiation at the *Escherichia coli* chromosomal origin. *Curr. Opin. Chem. Biol.* **15**, 606–613
4. Skarstad, K., and Katayama, T. (2013) Regulating DNA replication in bacteria. *Cold Spring Harb. Perspect. Biol.* **5**, a012922
5. Costa, A., Hood, I. V, and Berger, J. M. (2013) Mechanisms for initiating cellular DNA

replication. *Annu. Rev. Biochem.* **82**, 25–54

6. Ozaki, S., Noguchi, Y., Hayashi, Y., and Katayama, T. (2012) Differentiation of the DnaA-*oriC* subcomplex for DNA unwinding in a replication initiation complex. *J. Biol. Chem.* **287**, 37458–37471
7. Noguchi, Y., Sakiyama, Y., Kawakami, H., and Katayama, T. (2015) The Arg fingers of key DnaA protomers are oriented inward within the replication origin *oriC* and stimulate DnaA subcomplexes in the initiation complex. *J. Biol. Chem.* **290**, 20295–20312
8. Rozgaja, T. A., Grimwade, J. E., Iqbal, M., Czerwonka, C., Vora, M., and Leonard, A. C. (2011) Two oppositely oriented arrays of low-affinity recognition sites in *oriC* guide progressive binding of DnaA during *Escherichia coli* pre-RC assembly. *Mol. Microbiol.* **82**, 475–488
9. Ozaki, S., and Katayama, T. (2012) Highly organized DnaA-*oriC* complexes recruit the single-stranded DNA for replication initiation. *Nucleic Acids Res.* **40**, 1648–1665
10. Aeling, K. A., Opel, M. L., Steffen, N. R., Tretyachenko-Ladokhina, V., Hatfield, G. W., Lathrop, R. H., and Senear, D. F. (2006) Indirect recognition in sequence-specific DNA binding by *Escherichia coli* integration host factor: the role of DNA deformation energy. *J. Biol. Chem.* **281**, 39236–39248
11. Felczak, M. M., Simmonst, L. A., and Kaguni, J. M. (2005) An essential tryptophan of *Escherichia coli* DnaA protein functions in oligomerization at the *E. coli* replication origin. *J. Biol. Chem.* **280**, 24627–24633
12. Abe, Y., Jo, T., Matsuda, Y., Matsunaga, C., Katayama, T., and Ueda, T. (2007) Structure and function of DnaA N-terminal domains: specific sites and mechanisms in inter-DnaA interaction and in DnaB helicase loading on *oriC*. *J. Biol. Chem.* **282**, 17816–17827
13. Kawakami, H., Keyamura, K., and Katayama, T. (2005) Formation of an ATP-DnaA-specific initiation complex requires DnaA Arginine 285, a conserved motif in the AAA+ protein family. *J. Biol. Chem.* **280**, 27420–27430
14. Kawakami, H., Ozaki, S., Suzuki, S., Nakamura, K., Senriuchi, T., Su'etsugu, M., Fujimitsu, K., and Katayama, T. (2006) The exceptionally tight affinity of DnaA for ATP/ADP requires a unique aspartic acid residue in the AAA+ sensor I motif. *Mol. Microbiol.* **62**, 1310–1324
15. Nishida, S., Fujimitsu, K., Sekimizu, K., Ohmura, T., Ueda, T., and Katayama, T. (2002) A nucleotide switch in the *Escherichia coli* DnaA protein initiates chromosomal replication: evidnece from a mutant DnaA protein defective in regulatory ATP hydrolysis *in vitro* and *in vivo*. *J. Biol. Chem.* **277**, 14986–14995
16. Felczak, M. M., and Kaguni, J. M. (2004) The box VII motif of *Escherichia coli* DnaA protein is required for DnaA oligomerization at the *E. coli* replication origin. *J. Biol. Chem.* **279**, 51156–51162
17. Fujikawa, N., Kurumizaka, H., Nureki, O., Terada, T., Shirouzu, M., Katayama, T., and Shigeyuki, Y. (2003) Structural basis of replication origin recognition by the DnaA protein. *Nucleic Acids Res.* **31**, 2077–2086

18. Baker, T. A., and Kornberg, A. (1988) Transcriptional activation of initiation of replication from the *E. coli* chromosomal origin: An RNA-DNA hybrid near *oriC*. *Cell*. **55**, 113–123
19. von Freiesleben, U., and Rasmussen, K. V. (1992) The level of supercoiling affects the regulation of DNA replication in *Escherichia coli*. *Res. Microbiol.* **143**, 655–663
20. Holloman, W. K. (1976) Recombination promoted by superhelical DNA and the *recA* gene of *Escherichia coil*. *Proc. Natl. Acad. Sci. U. S. A.* **73**, 3910–3914
21. Travers, A., and Muskhelishvili, G. (2005) DNA supercoiling - a global transcriptional regulator for enterobacterial growth? *Nat. Rev. Microbiol.* **3**, 157–169
22. Dorman, C. J. (1996) Flexible response: DNA supercoiling, transcription and bacterial adaptation to environmental stress. *Trends Microbiol.* **4**, 214–216
23. Cheung, K. J., Badarinarayana, V., Selinger, D. W., Janse, D., and Church, G. M. (2003) A microarray-based antibiotic screen identifies a regulatory role for supercoiling in the osmotic stress response of *Escherichia coli*. *Genome Res.* 10.1101/gr.401003.
24. Blot, N., Mavathur, R., Geertz, M., Travers, A., and Muskhelishvili, G. (2006) Homeostatic regulation of supercoiling sensitivity coordinates transcription of the bacterial genome. *EMBO Rep.* **7**, 710–715
25. Lal, A., Dhar, A., Trostel, A., Kouzine, F., Seshasayee, A. S., and Adhya, S. (2016) Genome scale patterns of supercoiling in a bacterial chromosome. *Nat. Commun*. **7**, 11055
26. Cagliero, C., and Jin, D. J. (2013) Dissociation and re-association of RNA polymerase with DNA during osmotic stress response in *Escherichia coli*. *Nucleic Acids Res.* **41**, 315–326
27. Donczew, R., Mielke, T., Jaworski, P., Jolanta, Z.-C., and Zawilak-Pawlik, A. (2014) Assembly of *Helicobacter pylori* initiation complex is determined by sequence-specific and topology-sensitive DnaA-*oriC* interactions. *J. Mol. Biol.* **4**, 2769–2782
28. Riber, L., Frimodt-Møller, J., Charbon, G., and Løbner-Olesen, A. (2016) Multiple DNA binding proteins contribute to timing of chromosome replication in *E. coli*. *Front. Mol. Biosci.* **3**, 1–9
29. Kato, J., and Katayama, T. (2001) Hda, a novel DnaA-related protein, regulates the replication cycle in *Escherichia coli*. *EMBO J.* **20**, 4253–4262
30. Nakamura, K., and Katayama, T. (2010) Novel essential residues of Hda for interaction with DnaA in the regulatory inactivation of DnaA: unique roles for Hda AAA Box VI and VII motifs. *Mol. Microbiol.* **76**, 302–317
31. Camara, J. E., Breier, A. M., Brendler, T., Austin, S., Cozzarelli, N. R., and Crooke, E. (2005) Hda inactivation of DnaA is the predominant mechanism preventing hyperinitiation of *Escherichia coli* DNA replication. *EMBO Rep.* **6**, 736–741
32. Fujimitsu, K., Su'etsugu, M., Yamaguchi, Y., Mazda, K., Fu, N., Kawakami, H., and Katayama, T. (2008) Modes of overinitiation, *dnaA* gene expression, and inhibition of cell division in a novel cold-sensitive *hda* mutant of *Escherichia coli*. *J. Bacteriol.* **190**, 5368–5381
33. Kasho, K., and Katayama, T. (2013) DnaA binding locus *datA* promotes DnaA-ATP hydrolysis to enable cell cycle-coordinated replication initiation. *Proc. Natl. Acad. Sci. U. S. A.*

110, 936–941

34. Kitagawa, R., Ozaki, T., Moriya, S., and Ogawa, T. (1998) Negative control of replication initiation by a novel chromosomal locus exhibiting exceptional affinity for *Escherichia coli* DnaA protein. *Genes Dev.* **12**, 3032–3043
35. Nozaki, S., Yamada, Y., and Ogawa, T. (2009) Initiator titration complex formed at datA with the aid of IHF regulates replication timing in *Escherichia coli*. *Genes to cells*. **14**, 329–341
36. Ogawa, T., Yamada, Y., Kuroda, T., Kishi, T., and Moriya, S. (2002) The *datA* locus predominantly contributes to the initiator titration mechanism in the control of replication initiation in *Escherichia coli*. *Mol. Microbiol.* **44**, 1367–1375
37. Kasho, K., Fujimitsu, K., Matoba, T., Oshima, T., and Katayama, T. (2014) Timely binding of IHF and Fis to *DARS2* regulates ATP-DnaA production and replication initiation. *Nucleic Acids Res.* **42**, 13134–13149
38. Inoue, Y., Tanaka, H., Kasho, K., Fujimitsu, K., Oshima, T., and Katayama, T. (2016) Chromosomal location of the DnaA-reactivating sequence *DARS2* is important to regulate timely initiation of DNA replication in *Escherichia coli*. *Genes to Cells*. 10.1111/gtc.12395
39. Skarstad, K., and Boye, E. (1994) The initiator protein DnaA: evolution, properties and function. *Biochim. Biophys. Acta.* **1217**, 111–130
40. Su'etsugu, M., Emoto, A., Fujimitsu, K., Keyamura, K., and Katayama, T. (2003) Transcriptional control for initiation of chromosomal replication in *Escherichia coli*: Fluctuation of the level of origin transcription ensures timely initiation. *Genes to Cells*. **8**, 731–745
41. Skarstad, K., Løbner-Olesen, A., Atlung, T., von Meyenburg, K., and Boye, E. (1989) Initiation of DNA replication in *Escherichia coli* after overproduction of the DnaA protein. *Mol. Gen. Genet.* **218**, 50–56
42. Weigel, C., Messer, W., Preiss, S., Welzeck, M., Morigen, and Boye, E. (2001) The sequence requirements for a functional *Escherichia coli* replication origin are different for the chromosome and a minichromosome. *Mol. Microbiol.* **40**, 498–507
43. Kitagawa, R., Mitsuki, H., Okazaki, T., and Ogawa, T. (1996) A novel DnaA protein-binding site at 94.7 min on the *Escherichia coli* chromosome. *Mol. Microbiol.* **19**, 1137–1147
44. Morigen, Løbner-Olesen, A., and Skarstad, K. (2003) Titration of the *Escherichia coli* DnaA protein to excess *datA* sites causes destabilization of replication forks, delayed replication initiation and delayed cell division. *Mol. Microbiol.* **50**, 349–362
45. Morigen, Skarstad, K., and Molina, F. (2005) Deletion of the *datA* site does not affect once-per-cell-cycle timing but induces rifampin-resistant replication. *J. Bacteriol.* **187**, 3913–3920
46. Morigen, M., Flåtten, I., and Skarstad, K. (2014) The *Escherichia coli datA* site promotes proper regulation of cell division. *Microbiology*. **160**, 703–710
47. Sekimizu, K., Bramhill, D., and Kornberg, A. (1987) ATP activates *dnaA* protein in initiating replication of plasmids bearing the origin of the *E. coli* chromosome. *Cell*. **50**, 259–265

48. Erzberger, J. P., Mott, M. L., and Berger, J. M. (2006) Structural basis for ATP-dependent DnaA assembly and replication-origin remodeling. *Nat. Struct. Mol. Biol.* **13**, 676–683
49. Su'etsugu, M., Kawakami, H., Kurokawa, K., Kubota, T., Takata, M., and Katayama, T. (2001) DNA replication-coupled inactivation of DnaA protein *in vitro*: A role for DnaA arginine-334 of the AAA+ Box VIII motif in ATP hydrolysis. *Mol. Microbiol.* **40**, 376–386
50. Cozzarelli, N. R. (1980) DNA Gyrase and the supercoiling of DNA. *Science.* **207**, 953–960
51. von Freiesleben, U., Rasmussen, K. V, Atlung, T., and Hansen, F. G. (2000) Rifampicin-resistant initiation of chromosome replication from *oriC* in *ihf* mutants. *Mol. Microbiol.* **37**, 1087–1093
52. Cameron, A. D. S., Stoebel, D. M., and Dorman, C. J. (2011) DNA supercoiling is differentially regulated by environmental factors and FIS in *Escherichia coli* and *Salmonella enterica*. *Mol. Microbiol.* **80**, 85–101
53. Duggin, I. G., Wake, R. G., Bell, S. D., and Hill, T. M. (2008) The replication fork trap and termination of chromosome replication. *Mol. Microbiol.* **70**, 1323–1333
54. Peter, B. J., Arsuaga, J., Breier, A. M., Khodursky, A. B., Brown, P. O., and Cozzarelli, N. R. (2004) Genomic transcriptional response to loss of chromosomal supercoiling in *Escherichia coli*. *Genome Biol.* **5**, R87
55. Sheridan, S. D., Benham, C. J., and Hatfield, G. W. (1998) Activation of gene expression by a novel DNA structural transmission mechanism that requires supercoiling-induced DNA duplex destabilization in an upstream activating sequence. *J. Biol. Chem.* **273**, 21298–21308
56. Teter, B., Goodman, S. D., and Galas, D. J. (2000) DNA bending and twisting properties of integration host factor determined by DNA cyclization. *Plasmid*. **84**, 73–84
57. Drlica, K., Franco, R. J., and Steck, T. R. (1988) Rifampin and *rpoB* mutations can alter DNA supercoiling in *Escherichia coli*. *J. Bacteriol.* **170**, 4983–4985
58. Weigel, C., Schmidt, A., Lurz, R., and Messer, W. (1997) DnaA protein binding to individual DnaA boxes in the *Escherichia coli* replication origin, *oriC*. *EMBO J.* **16**, 6574–6583
59. Krause, M., Ru, B., Lurz, R., and Messer, W. (1997) Complexes at the replication origin of *Bacillus subtilis* with homologous and heterologous DnaA protein. *J. Mol. Biol.* **274**, 365–380
60. Remus, D., Beall, E. L., and Botchan, M. R. (2004) DNA topology, not DNA sequence, is a critical determinant for *Drosophila* ORC–DNA binding. *EMBO J.* **23**, 897–907
61. Okumura, H., Yoshimura, M., Ueki, M., Oshima, T., Ogasawara, N., and Ishikawa, S. (2012) Regulation of chromosomal replication initiation by *oriC*-proximal DnaA-box clusters in *Bacillus subtilis*. *Nucleic Acids Res.* **40**, 220–234
62. Smulczyk-Krawczyszyn, A., Jakimowicz, D., Ruban-Osmialowska, B., Zawilak-Pawlik, A., Majka, J., Chater, K., and Zakrzewska-Czerwinska, J. (2006) Cluster of DnaA boxes involved in regulation of *Streptomyces* chromosome replication: from *in silico* to *in vivo* studies. *J. Bacteriol.* **188**, 6184–6194
63. Teyssier, C., Toulme, F., Touzel, J., Gervais, A., and Maurizot, J. (1996) Preferential binding of the archaebacterial histone-like MC1 protein to negatively supercoiled DNA minicircles.

Biochemistry. **2960**, 7954–7958

64. Štros, M., and Reich, J. (1998) Formation of large nucleoprotein complexes upon binding of the high-mobility-group (HMG) box B-domain of HMG1 protein to supercoiled DNA. *Eur. J. Biochem.* **251**, 427–434

65. Datsenko, K. A., and Wanner, B. L. (2000) One-step inactivation of chromosomal genes in *Escherichia coli* K-12 using PCR products. *Proc. Natl. Acad. Sci. U. S. A.* **97**, 6640–6645

FOOTNOTES

This study was supported by the Grant-in-Aid for Scientific Research (KAKENHI no. 15K18479, 26291004, 26650127, and 16H00775) from the Ministry of Education, Culture, Sports, Science and Technology of Japan and the Japan Society for the Promotion of Science and by the Kyushu University Qdai-jump Research Program (Former Interdisciplinary Programs in Education and Projects in Research Development) (no. 26122, and 28247) and English/Japanese Proofreading Expenses Support.

FIGURE LEGENDS

FIGURE 1. Inter-DnaA interaction modes on *oriC* and *datA*.

A, Schematic presentation of the *oriC* and *datA* structure. The upper open bar indicates the minimal *oriC* (245 bp) for replication initiation. Black arrowheads and a green bar represent 9 bp DnaA boxes (consensus sequence: TTATNCACA, where N is any nucleotide) and IHF-binding site (IBS; consensus sequence: TAANNNNTTGATW, where W is A or T), respectively. *oriC* contains two high-affinity DnaA boxes, termed R1 and R4, and a number of moderate- or low-affinity DnaA boxes. The lower open bar indicates the wild-type *datA* region. Black arrowheads and a green bar represent 9 bp DnaA boxes and IBS, respectively. *datA* (991 bp) contains five known DnaA boxes, termed DnaA boxes 1–5. A 262 bp region including IBS and DnaA boxes 2 and 3 is indicated.

B, Inter-DnaA interaction in the ATP-DnaA oligomers on *oriC* and *datA*. For simplicity, only domain III of two ATP-DnaA protomers is represented. DnaA domain III contains inter-DnaA interaction motifs (AID-1 Arg227 and AID-2 Leu290, arginine-finger Arg285, Box VII Arg281), and an ATP-hydrolyzing motif (Sensor II Arg334). In the ATP-DnaA-*oriC* complexes, ATP-DnaA tightly interacts with all inter-DnaA interaction motifs. In the ATP-DnaA-*datA* complexes, Arg285 and Arg281 are thought to recognize the neighboring DnaA protomer and promote the interaction between ATP and Arg334, whereas the roles of AID-1/2 are unidentified. These motifs are indicated by different colors and the same colors are used for the same motifs in the two promoters

FIGURE 2. *datA* DnaA box 7 is essential for DDAH *in vitro*.

A, Detail of the uncharacterized *datA* DnaA boxes 6 and 7. Nucleotide sequence spanning a region from DnaA box 1 to DnaA box 2 is shown below. DnaA boxes 1 and 2, as well as potential DnaA boxes 6 and 7, are indicated by black and grey arrows, respectively.

B, Mutational analyses of DnaA boxes 6 and 7. [α-^{32}P]ATP-DnaA (1 pmol) was incubated at 30°C for 10 min in buffer containing IHF (0.5 pmol), and 50 fmol or 100 fmol PCR fragments harboring *datA* (991 bp) (wild type (WT), or containing substitutions in box 1 (subDnaAbox1), box 6 (subDnaAbox6), box 7 (subDnaAbox7), or box 2 (subDnaAbox2)) or *oriC* in the presence of 100 mM NaCl. The proportions of ADP-DnaA to the total ATP/ADP-DnaA are indicated as percentages [%].

C–F, Requirement for DnaA box 7 for DnaA oligomerization on *datA*. (*C*) The black bar indicates the *datA* del5 fragment (262 bp) and *datA* 672 fragment (43 bp) used in EMSA. (*D*) The indicated amounts of ATP-DnaA or ADP-DnaA were incubated with *datA* del5 or *datA* del5 with the subDnaAbox7 mutation (150 fmol), along with IHF (6 pmol), and 150 ng λDNA (as a competitor) at 15°C for 5 min, followed by EMSA with a 2% agarose gel and ethidium-bromide staining. The gel images are shown in black-and-white inverted mode, with ordinary contrast (*upper*) and higher contrast for better visibility of topoisomers (*lower*). "IHF" indicates IHF-bound *datA*, "C1–C4" indicates the lower *datA*-IHF complexes with 1–4 DnaA molecules, "≥C5" indicates higher *datA*-IHF complexes with more than five DnaA molecules. The proportions of higher (*E*; ≥C5; ●, ○) and lower complexes (*F*; C1–C4; ▲, △) of ATP-DnaA (●, ▲) or ADP-DnaA (○, △) were determined using the data shown in C and are plotted as percentages.

G, Cooperative DnaA binding to DnaA boxes 6 and 7 with neighboring DnaA box 2. The indicated amounts of ATP-DnaA were incubated with derivatives of *datA* 672 fragment (WT, or with the subDnaAbox6, subDnaAbox7, or subDnaAbox2 mutations; 43 bp, 500 fmol) at 30°C for 5 min, followed by EMSA with 8% PAGE.

FIGURE 3. DnaA motifs are required for formation of DDAH-active ATP-DnaA-specific oligomers on *datA*.

A, [α-^{32}P]ATP-DnaA (wild type (WT), R227A, or L290A; 1 pmol) was incubated at 30°C for 10 min in buffer containing IHF (0.5 pmol), and 100 fmol of PCR fragments harboring *datA* wild type, as described in Fig. 2*B*.

B–J, Oligomerization of DnaA mutants on *datA*. (*B*) The indicated amounts of ATP-DnaA or ADP-DnaA (WT or L290A) were incubated with *datA* del5 wild type, as described in Fig. 2*D*. The proportions of higher (*C*) and lower (*D*) complexes of ATP-DnaA or ADP-DnaA were determined, as described in Fig. 2, *E* and *F*. Similar experiments were performed using DnaA R285A (*E–G*) and R281A (*H–J*).

FIGURE 4. *datA* DnaA box 7 is essential for repression of replication initiation *in vivo*.

A, Flow cytometry analysis of *datA* DnaA box 7 mutant plasmid. MG1655 cells bearing pACYC177 (vector), pKX40 (*datA* wild type), or the indicated pKX40-derivative *datA* mutant plasmids were cultivated at 37°C in LB medium containing 50 μg/ml ampicillin and analyzed by flow cytometry.

Doubling time, ratios of mean cell mass and ori/mass, and asynchrony index are shown with histograms of chromosome counts.

B and *C*, Flow cytometry analysis of chromosomal *datA* DnaA-box mutant cells. SR01 (wild type), MIT128 (Δ*datA*::*kan*), SR10 (subDnaAbox6), SR30 (subDnaAbox7), and SR06 (subDnaAbox2) cells were cultivated at 37°C in LB (*B*) or supplemented M9 medium (*C*) and analyzed by flow cytometry.

FIGURE 5. DNA supercoiling-dependent stabilization of DDAH.

A, Basic structure of supercoiled (SC) and linear (Lin) forms of *datA*-harboring plasmids. pKX40, a pACYC177-based plasmid harboring the *datA* WT fragment (991 bp), was used for analysis of DDAH activity.

B and *C*, Salt-resistant DDAH with supercoiled pKX40. [α-^{32}P]ATP-DnaA (1 pmol) was incubated at 30°C for 10 min in buffer containing IHF (0.25 pmol), the supercoiled (*B*) or linear forms (*C*) of pKX40 or pACYC177, and 100, 150, or 200 mM NaCl. The proportions of ADP-DnaA to the total ATP/ADP-DnaA are indicated as percentages [%].

D, DDAH activities of supercoiled and linear pKX40 in the presence of 150 mM NaCl. [α-^{32}P]ATP-DnaA (1 pmol) was incubated at 30°C for 10 min with the indicated amounts of supercoiled (SC; ●, ○) or linear forms (Lin; ▲, △) of pKX40 (+; ●, ▲) or pACYC177 (-; ○, △) in buffer containing 150 mM NaCl and 0.25 pmol IHF.

E, Time course of DDAH. Experiments similar to those shown in *panel D* were performed using 25 fmol supercoiled (SC; ●, ○) or linear forms (Lin; ▲, △) of pKX40 (+; ●, ▲) or pACYC177 (-; ○, △) and 0.25 pmol IHF.

F, Requirement for IHF in DDAH of supercoiled pKX40. [α-^{32}P]ATP-DnaA was incubated with the indicated amounts of IHF with 25 fmol supercoiled (SC; ●, ○) or linear forms (Lin; ▲, △) of pKX40 (+; ●, ▲) or pACYC177 (-; ○, △).

FIGURE 6. Specific DnaA boxes and IBS are required for DDAH promoted by supercoiled *datA*.

A, Deletion analysis of supercoiled *datA*. The open bar at the top depicts the *datA* region, as described in Fig. 1A. The supercoiled form (25 fmol) of pKX40 (WT *datA*) and its derivatives that bear a truncated *datA* region (black bar) were incubated at 30°C for 10 min with [α-^{32}P]ATP-DnaA (1 pmol) and IHF (0.25 pmol), followed by analysis of DnaA-bound nucleotides, as described in Fig. 5*B*. Results [%] are shown on the right of the bars.

B, Analysis of *datA* substitution mutants. Similar experiments were performed using the indicated substitution mutants of *datA* on supercoiled pKX40. subDnaAbox1–7 or subIBS contain substitutions of the corresponding DnaA boxes and IBS, as described in Fig. 2*B* and the previous report (33).

FIGURE 7. Requirements for specific DnaA motifs in DDAH with supercoiled *datA*.

A and *B*, Analysis of AID-motifs. The [α-^{32}P]ATP forms (1 pmol) of DnaA wild type (WT) (●, ○), R227A (▲, △), and L290A (■, □) were incubated at 30°C for 10 min with IHF (0.25 pmol), and the

indicated amounts of supercoiled (*A*) or linear forms (*B*) of pKX40 (+; ●, ▲, ■) or pACYC177 (-; ○, △, □).

C and *D*, Analysis of arginine-fingers. Similar experiments were performed using DnaA WT (●, ○), R285A (■, □), and R281A (▲, △) using the supercoiled (*C*) or linear forms (*D*) of pKX40 (+; ●, ▲, ■) or pACYC177 (-; ○, △, □).

E and *F*, Analysis of sensor II-motif. Similar experiments were performed using DnaA WT (●, ○) or R334A (▲, △) using the supercoiled (*E*) or linear forms (*F*) of pKX40 (+; ●, ▲) or pACYC177 (-; ○, △).

FIGURE 8. DNA supercoiling stabilizes DnaA oligomerization and IHF binding on *datA*.

A, Primary structure of the *datA* mutant containing BglII-recognition site between IBS and DnaA box 3. The substituted site is shown below the *datA* wild-type (WT) sequence, and the substituted bases are shown in red.

B and *C*, BglII-protection assay for DnaA oligomerization. The indicated amounts of ATP-DnaA were incubated with supercoiled (SC; ●) or linear forms (Lin; ▲) of pKX133 at 30°C for 30 min in buffer containing 100 mM NaCl in the presence of BglII (2.5 U). The proportion of undigested DNA to total DNA is indicated as percentages [%] (*B*). Similar experiments were performed at 30°C for 45 min in buffer containing 150 mM NaCl (*C*).

D, Structure of the *datA* IBS_{EcoRV} mutant. The EcoRV recognition sequence, GATATC, was introduced by substituting the two bases adjacent to IBS.

E, IHF binding to the IBS_{EcoRV} site. The indicated amounts of IHF were incubated at 30°C for 5 min with *datA* del5 or its derivatives bearing IBS_{EcoRV}, or ΔIBS sequence (100 fmol) in buffer containing 150 mM NaCl, followed by 5% PAGE.

F and *G*, EcoRV-protection assay for IHF binding. The indicated amounts of IHF were incubated with supercoiled (SC; ●) or linear forms (Lin; ▲) of pHT25 at 30°C for 5 min in buffer containing 100 mM NaCl in the presence of EcoRV (0.5 U). The proportion of undigested DNA to the total DNA is indicated as percentages [%] (*F*). Similar experiments were performed in buffer containing 150 mM NaCl (*G*).

FIGURE 9. Modulation of DNA supercoiling decreases *datA* function *in vivo*.

A, Suppression of *datA*-dependent growth inhibition by novobiocin. Strains MG1655 (WT) and KMG-5 (Δ*ihfA*) were transformed with pBR322 (vector) or pKX88 (*datA*) and incubated at 37°C for 12 h on NaCl-depleted LB agar plates containing 50 μg/ml ampicillin and 0 or 15 μg/ml novobiocin (Novo). Colony formation with each set of cells is shown.

B and *C*, Suppression of *datA*-dependent repression of replication initiation by novobiocin. (*B*) MG1655 or KMG-5 cells harboring pBR322 or pKX88 were cultivated at 37°C in NaCl-depleted LB medium containing 50 μg/ml ampicillin and 0 or 15 μg/ml novobiocin (Novo), and analyzed by flow cytometry. (*C*) Mean cell mass and the ori/mass ratio (relative to MG1655 cells with pBR322) are shown in the histograms.

D, Relaxation of plasmid by addition of novobiocin. 50 ng of pBR322 topoisomers collected from cells cultivated in NaCl-depleted LB containing 50 μg/ml ampicillin and 0 or 15 μg/ml novobiocin (Novo) were separated by 0.65% (w/v) agarose-gel electrophoresis, and stained by ethidium bromide. The gel image is shown in black-and-white inverted mode.

E, Relative copy number of plasmid DNA. The cultures, prepared in the experiments shown in Fig. 9*D*, were boiled, and supernatants were collected. The ratio of pBR322 *tet* gene per chromosomal *terC* locus in the supernatants was determined using quantitative PCR. Duplicated samples were used in this experiment.

FIGURE 10. Molecular mechanism for activating DDAH.

A, Summary of the functional requirements of DnaA motifs for *oriC*, *datA*, *DARS1* and *DARS2*. For functional DnaA oligomerization in *oriC*, roles for AID motifs are different between the left-half (Left) and right-half (Right) subregions. +, essential. ±, stimulatory. −, non-essential. n.d., not determined. See text for references.

B, Mechanistic models of the DnaA–IHF–*datA* complex for activating DDAH. ATP-DnaA oligomers are formed on the *datA* minimal region containing DnaA boxes 7, 2, and 3. For simplicity, only DnaA domain III (blue or red polygons), the arginine finger (pink triangle), and domain IV (orange square) are shown. DnaA molecules bound to DnaA boxes 4 and 6 as well as additional DnaA molecules forming extended complexes are omitted. Negative DNA supercoiling stabilizes DnaA oligomerization and IHF binding on *datA*. Sharp DNA bending by IHF might stimulate the inter-molecular contact of oligomers formed around DnaA boxes 2 and 3. Cooperative ATP-DnaA binding on *datA* DnaA box 7 might induce conformational change of the DnaA nucleotide pocket to activate DnaA-ATP hydrolysis (Model 1). Alternatively, in the oligomer formed around DnaA box 2, DnaA-ATP hydrolysis might be activated by interaction with the oligomer formed around DnaA box 3 (Model 2). In both models, DnaA AID-2 Leu290 residue is important for ATP-DnaA-specific interactions, especially for destabilizing the resultant ADP-DnaA protomers to enable further binding and hydrolysis of ATP-DnaA. In the cartoon, DnaA domain III colored with blue, but not red, promotes hydrolysis of bound ATP.

Table 1. List of oligonucleotides

Primers	Sequences
subL1-U	GACAACAAAAACCAGCAATAACGC
subL1-L	ACATGTCTTCTCTTGTAAACAGAGTTATCCACAGCC
tnk126datAlow-F	CTCAGGCTGTAATCTTAATTTCAAAGAAACTTCGCACGGTG
tnk128datAlow-B	GCTGTGGATAACTCACATGTCTTGAGTTTGTCAGAGACAACAAA AACCAGCAATAACGC
40BglII-U	GAAGATCTCTTGACGATTTTATTCGTCTTGAATTG
40BglII-L	GAAGATCTACTCGACAAAACGGAATCTTAATTTTTAAC
tnk124IBSEcoRV-F	GTGAATAGTATTTTTTTAACCTATTGATATCTAAGTTAAAAATTA AGATTC
tnk125IBSEcoRV-R	CGTGCGAAGTTTCTTTGAAATTAAGATTACAGCCTG
datA-1	CCCGCTCCAAATTCTTCTCTCA
datA-2	TTCTCGAGCGCCCGTTAGCTG
datA-3	CAGCGTCTGGTTCGGGTG
datA-6	GTTGTCTCTGACAAACTCTTGTAAACAG
datA6subDnaAbox7	GTTGTCTCTGACAAACTCAAGACATGTG
datAEcoRI-U	CGGAATTCGAAGAATTTGGAGCGGGAGCTTATG
datAEcoRI-L	GCGAATTCTCTCAATAAAATATCCACAGCGACGC
672WT-U	TTGTCTCTGACAAACTCTTGTAAACAGAGTTATCCACAGCCTC
672WT-L	GAGGCTGTGGATAACTCTGTTTACAAGAGTTTGTCAGAGACAA
sub672-U	TTGTCACATGTATTCTCTTGTAAACAGAGTTATCCACAGCCTC
sub672-L	GAGGCTGTGGATAACTCTGTTTACAAGAGAATACATGTGACAA
6sub72-U	TTGTCTCTGACAAACTCAAGACATGTGAGTTATCCACAGCCTC
6sub72-L	GAGGCTGTGGATAACTCACATGTCTTGAGTTTGTCAGAGACAA
67sub2-U	TTGTCTCTGACAAACTCTTGTAAACAGAGAACATGTGTGCCTC
67sub2-L	GAGGCACACATGTTCTCTGTTTACAAGAGTTTGTCAGAGACAA
tnk116datA-3	CGGGATCCCAGCGTCTGGTTCGGGTG
tnk117datA-6	CCCAAGCTTGTTGTCTCTGACAAACTCTTGTAAACAG
tnk118datA-7	CCCAAGCTTGCCTCAGGCTGTAATCTTAATTTC
tnk119datA-9	CGGGATCCAAATAAAAACGCATTGCAATTC
tnk120datA-10	CGGGATCCAGCTTGTGAATAAAAATAAAAACGC
tnk121datA-1	CCCAAGCTTCCCGCTCCAAATTCTTCTCTCA
tnk122datA-2	CGGGATCCTTCTCGAGCGCCCGTTAGCTG
ChdatAKn	GTCGGGGTCGCGAGTTCGAGTCTCGTTTCCCGCTCCAAATTCTTC TCTCAGTGTAGGCTGGAGCTGCTTC
ChdatAsub6	TTACAGCCTGAGGCTGTGGATAACTCTGTTTACAAGAGAATACA

	TGTGACAACAAAAACCAGCAATAACG
ChdatAsub7	GAAATTAAGATTACAGCCTGAGGCTGTGGATAACTCACATGTCT
	TGAGTTTGTCAGAGACAACAAAAACC
ChdatAsub2	AAGTTTCTTTGAAATTAAGATTACAGCCTGAGGCACACATGTTCT
	CTGTTTACAAGAGTTTGTCAGAGAC
TER_2	TATCTTCCTGCTCAACGGTC
SUEterRev1	GAACTACGCGGGAAATACC
SMT-7	GGAGCTGACTGGGTTGAAGG
RTpBR322	CAACGGCCTCAACCTACTACTG

Table 2. List of *Escherichia coli* strains

Strain	Relevant genotype	Source
MG1655	wild type	Laboratory stock
SR01	wild-type *datA-frt*	This work
MIT128	Δ*datA::kan*	This work
SR10	*datA* subDnaAbox6-*frt*	This work
SR30	*datA* subDnaAbox7-*frt*	This work
SR06	*datA* subDnaAbox2-*frt*	This work
KMG-5	Δ*ihfA::frt-kan*	(32)

Figure 1

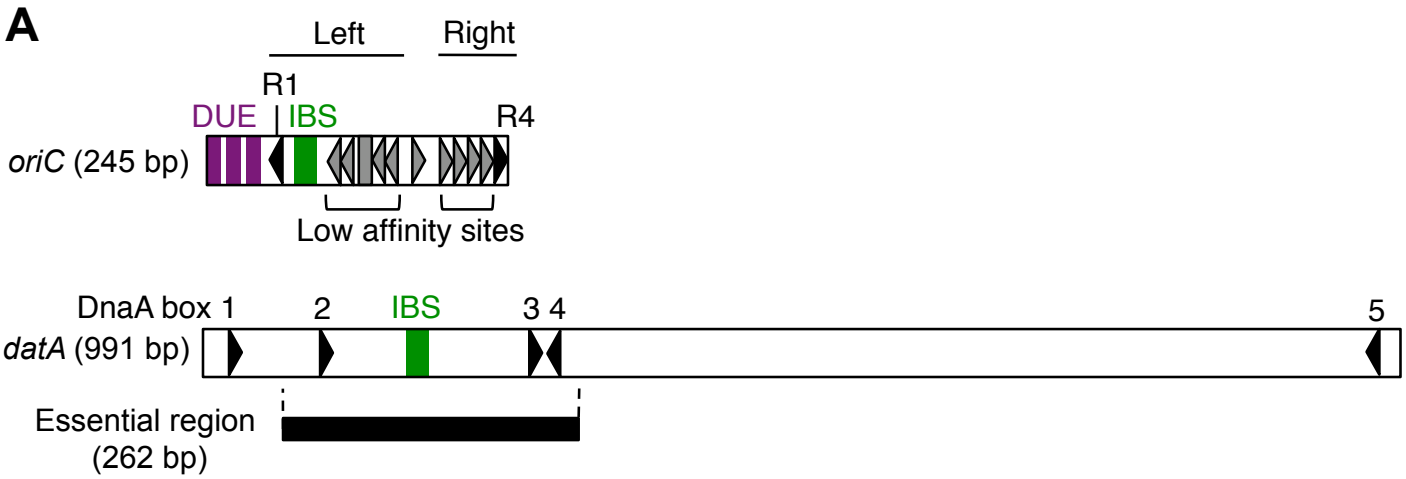
A
Left
Right
R1
DUE
IBS
R4
oriC (245 bp)
Low affinity sites
DnaA box 1
2
IBS
3 4
5
datA (991 bp)
Essential region
(262 bp)

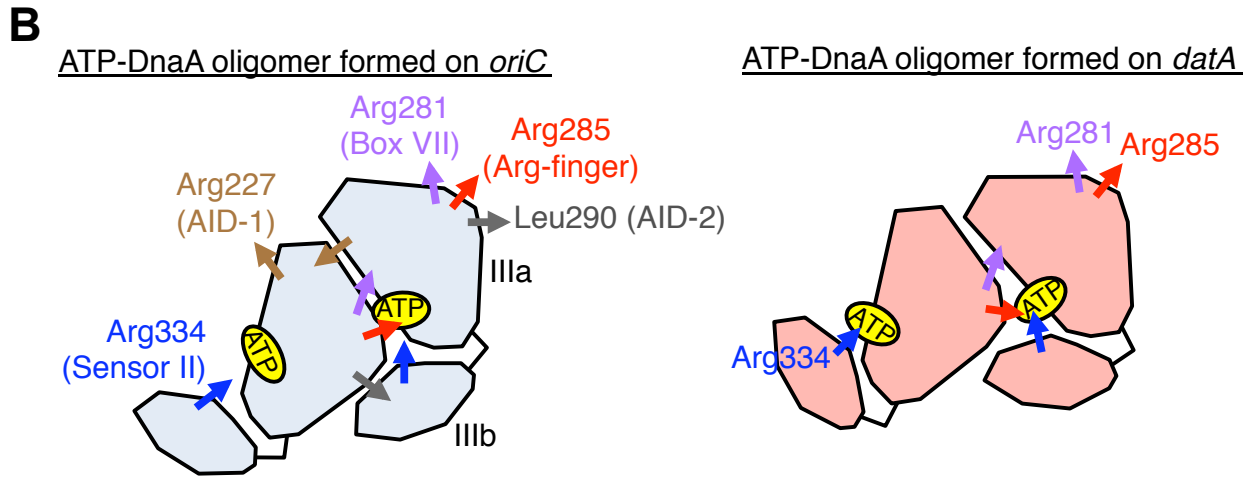
B
ATP-DnaA oligomer formed on oriC
Arg281
(Box VII)
Arg285
(Arg-finger)
Arg227
(AID-1)
Leu290 (AID-2)
IIIa
ATP
ATP
Arg334
(Sensor II)
IIIb
ATP-DnaA oligomer formed on datA
Arg281
Arg285
ATP
ATP
Arg334

Figure 2

A

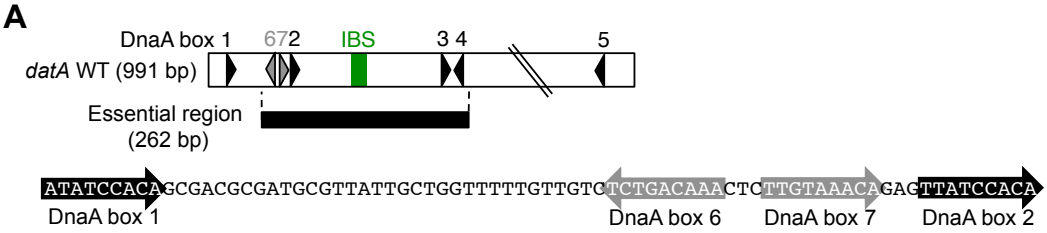

B

PCR fragments, 100 mM NaCl

DNA	Sequences		ADP/(ATP+ADP) on DnaA [%]	
	WT	Mutants	0.05 pmol	0.1 pmol
datA WT			80 ± 6	92 ± 8
subDnaAbox1	ATATCCACA	AATATGTGT	98 ± 2	ND
subDnaAbox6	TTTGTCAGA	AATACATGT	68 ± 3	95 ± 1
subDnaAbox7	TTGTAAACA	AAGACATGT	9.4 ± 0.1	10 ± 0
subDnaAbox2	TTATCCACA	AACATGTGT	ND	12 ± 0
FK-9 (*oriC*)			ND	11 ± 1
No DNA			9.0 ± 1.3	

C

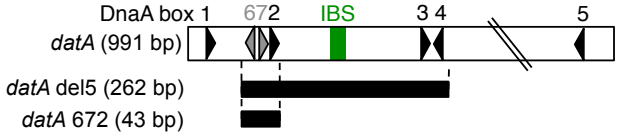

D

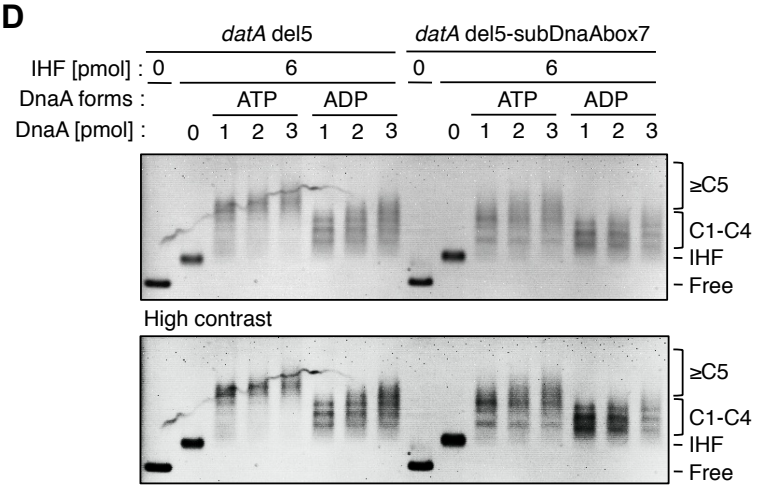

E

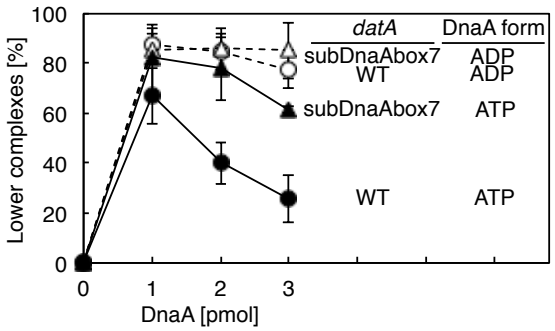

F

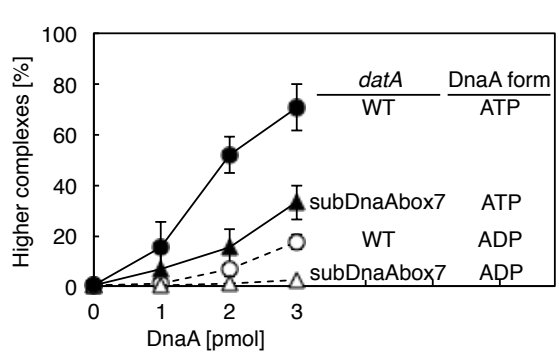

G

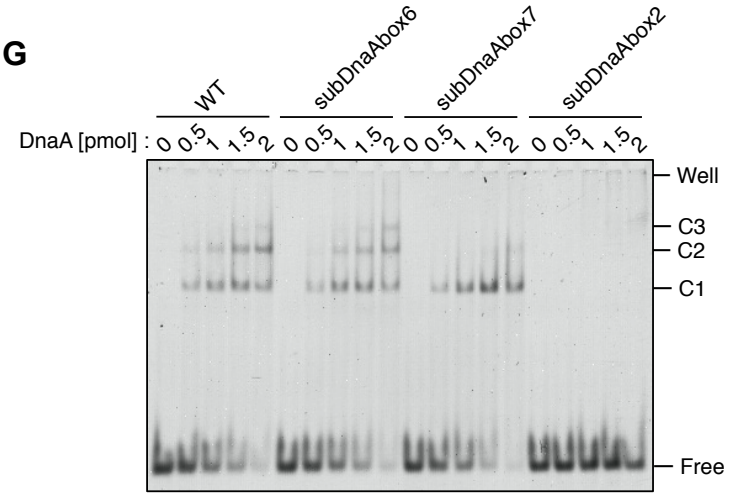

Figure 3

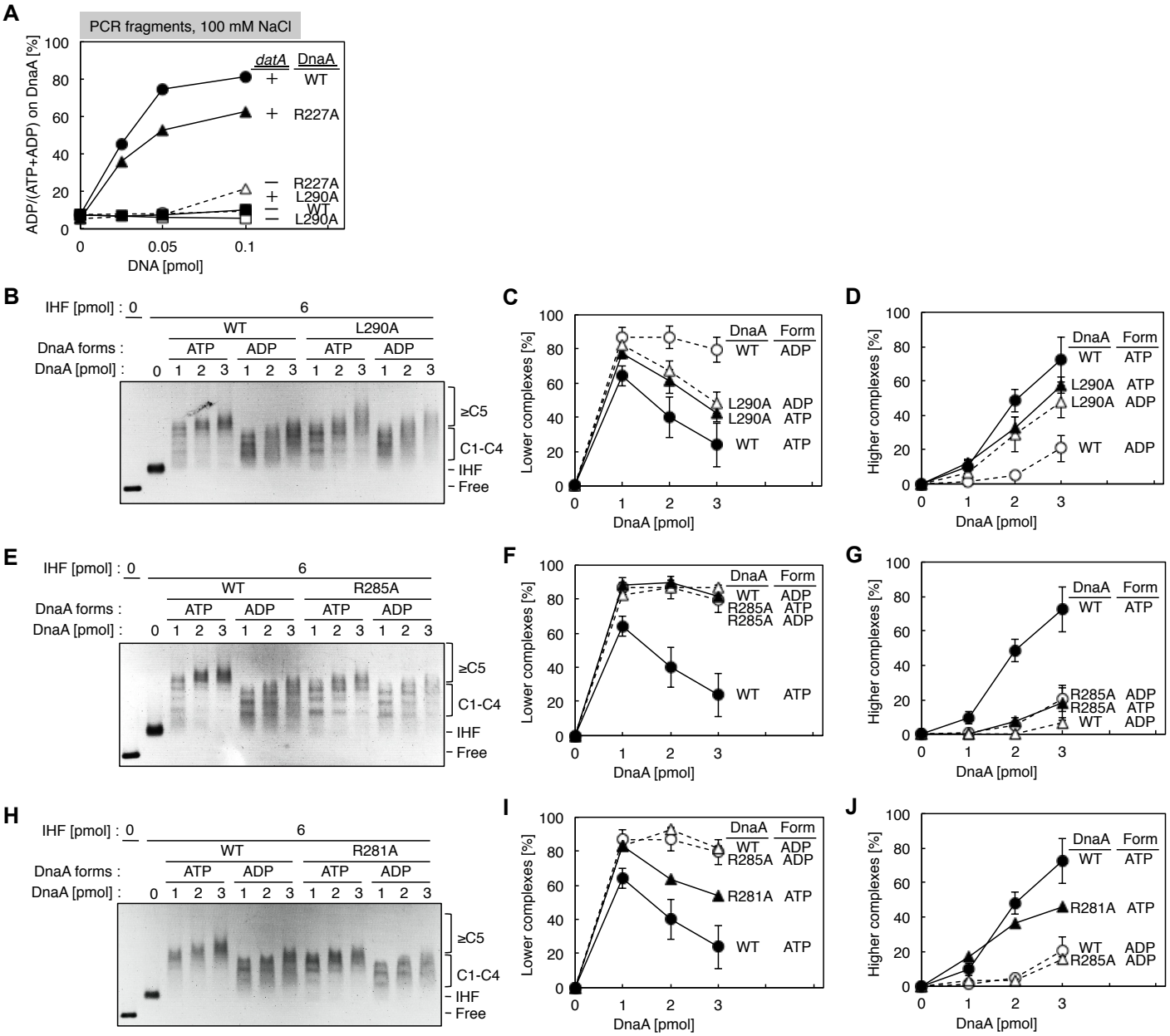
A
PCR fragments, 100 mM NaCl
ADP/(ATP+ADP) on DnaA [%]
DNA [pmol]
datA
DnaA
WT
R227A
R227A
L290A
WT
L290A
B
IHF [pmol] : 0 6
WT L290A
DnaA forms : ATP ADP ATP ADP
DnaA [pmol] : 0 1 2 3 1 2 3 1 2 3 1 2 3
≥C5
C1-C4
IHF
Free
C
Lower complexes [%]
DnaA [pmol]
DnaA Form
WT ADP
L290A ADP
L290A ATP
WT ATP
D
Higher complexes [%]
DnaA [pmol]
DnaA Form
WT ATP
L290A ATP
L290A ADP
WT ADP
E
IHF [pmol] : 0 6
WT R285A
DnaA forms : ATP ADP ATP ADP
DnaA [pmol] : 0 1 2 3 1 2 3 1 2 3 1 2 3
≥C5
C1-C4
IHF
Free
F
Lower complexes [%]
DnaA [pmol]
DnaA Form
WT ADP
R285A ATP
R285A ADP
WT ATP
G
Higher complexes [%]
DnaA [pmol]
DnaA Form
WT ATP
R285A ADP
R285A ATP
WT ADP
H
IHF [pmol] : 0 6
WT R281A
DnaA forms : ATP ADP ATP ADP
DnaA [pmol] : 0 1 2 3 1 2 3 1 2 3 1 2 3
≥C5
C1-C4
IHF
Free
I
Lower complexes [%]
DnaA [pmol]
DnaA Form
WT ADP
R285A ADP
R281A ATP
WT ATP
J
Higher complexes [%]
DnaA [pmol]
DnaA Form
WT ATP
R281A ATP
WT ADP
R285A ADP

Figure 4

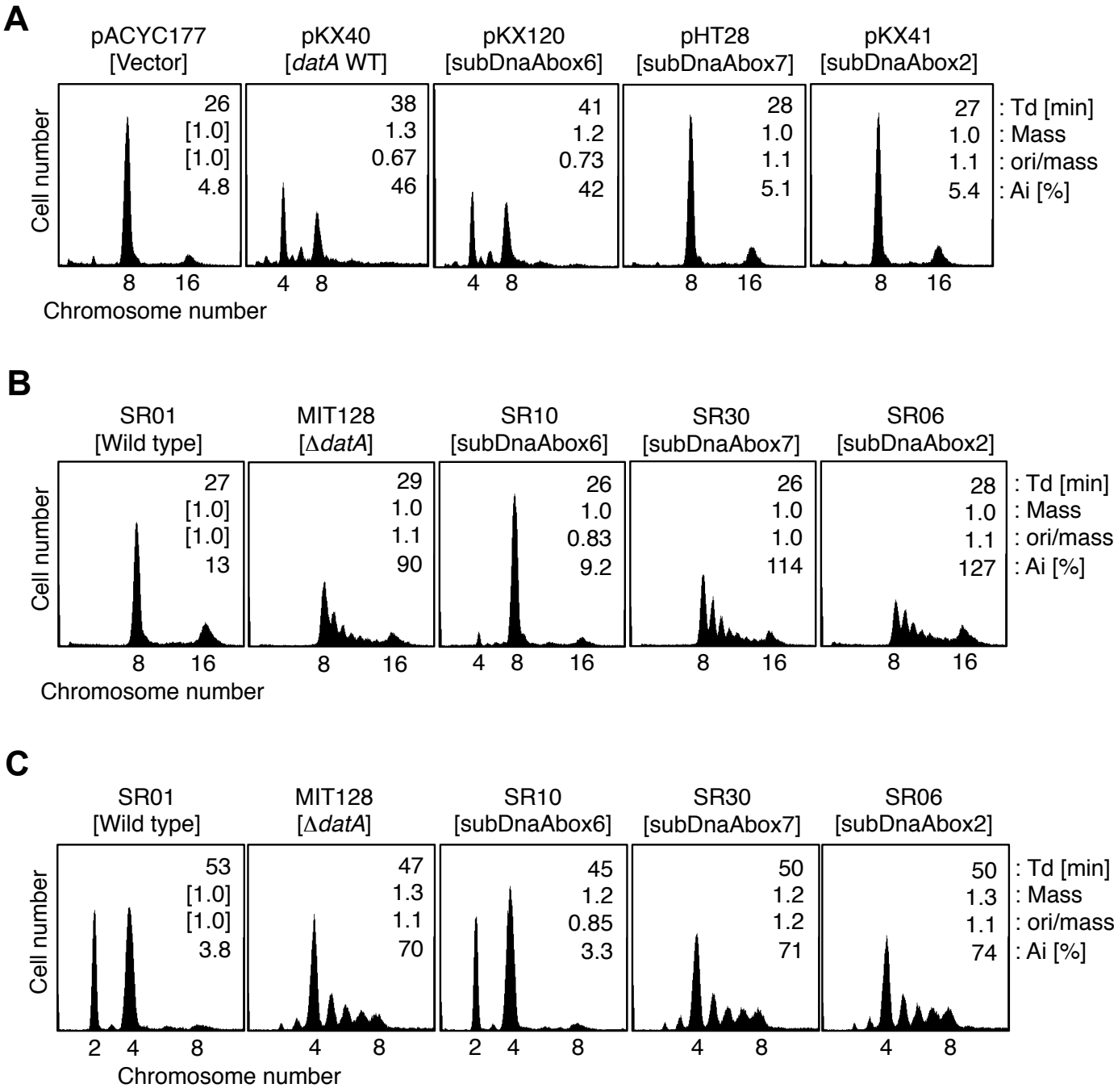
A
pACYC177
[Vector]
pKX40
[datA WT]
pKX120
[subDnaAbox6]
pHT28
[subDnaAbox7]
pKX41
[subDnaAbox2]
26
[1.0]
[1.0]
4.8
38
1.3
0.67
46
41
1.2
0.73
42
28
1.0
1.1
5.1
27
1.0
1.1
5.4
: Td [min]
: Mass
: ori/mass
: Ai [%]
Cell number
8 16
4 8
4 8
8 16
8 16
Chromosome number
B
SR01
[Wild type]
MIT128
[ΔdatA]
SR10
[subDnaAbox6]
SR30
[subDnaAbox7]
SR06
[subDnaAbox2]
27
[1.0]
[1.0]
13
29
1.0
1.1
90
26
1.0
0.83
9.2
26
1.0
1.0
114
28
1.0
1.1
127
: Td [min]
: Mass
: ori/mass
: Ai [%]
Cell number
8 16
8 16
4 8 16
8 16
8 16
Chromosome number
C
SR01
[Wild type]
MIT128
[ΔdatA]
SR10
[subDnaAbox6]
SR30
[subDnaAbox7]
SR06
[subDnaAbox2]
53
[1.0]
[1.0]
3.8
47
1.3
1.1
70
45
1.2
0.85
3.3
50
1.2
1.2
71
50
1.3
1.1
74
: Td [min]
: Mass
: ori/mass
: Ai [%]
Cell number
2 4 8
4 8
2 4 8
4 8
4 8
Chromosome number

Figure 5

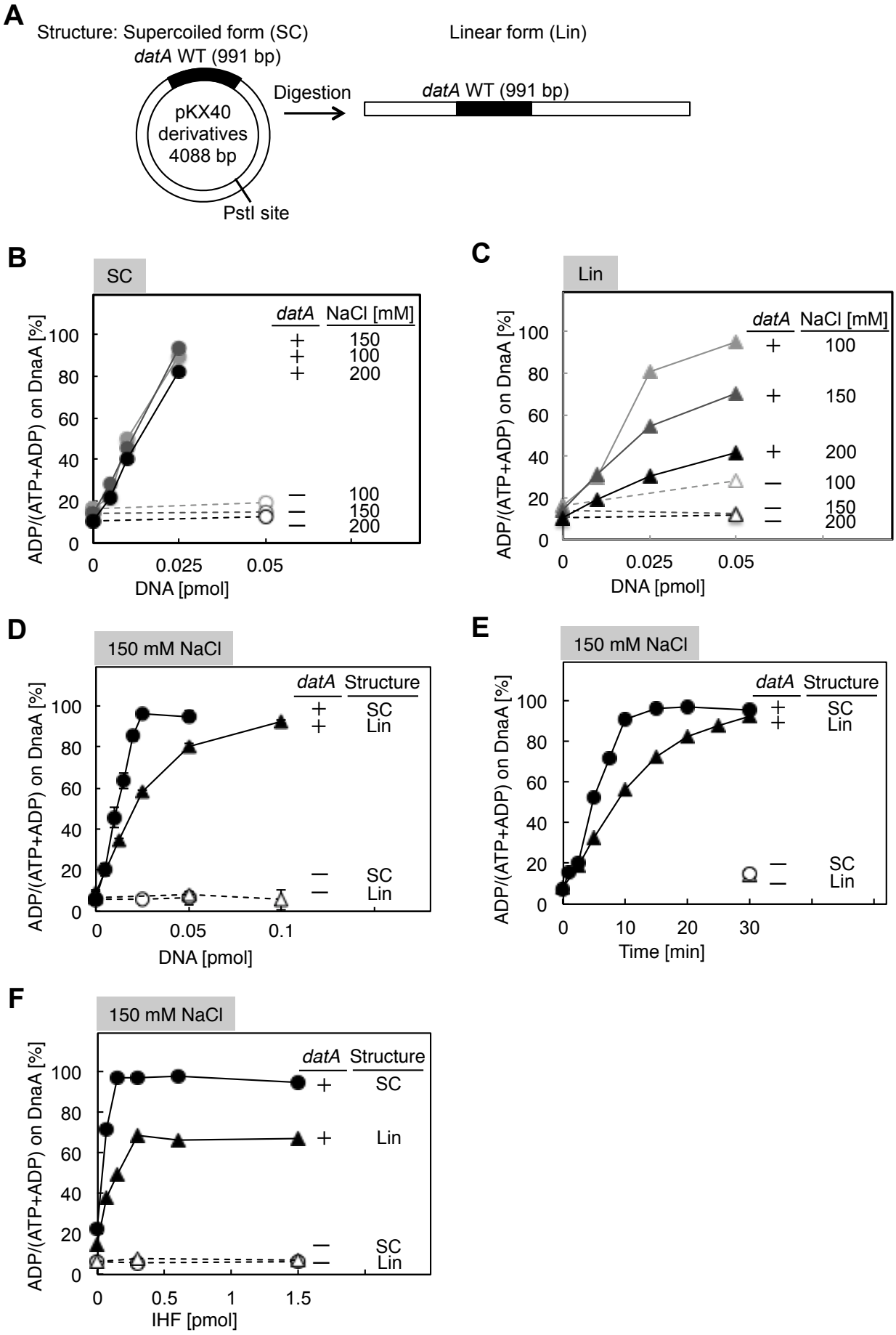
A
Structure: Supercoiled form (SC)
Linear form (Lin)
datA WT (991 bp)
pKX40 derivatives 4088 bp
PstI site
Digestion
datA WT (991 bp)
B
SC
datA
NaCl [mM]
+ 150
+ 100
+ 200
— 100
— 150
— 200
ADP/(ATP+ADP) on DnaA [%]
DNA [pmol]
C
Lin
datA
NaCl [mM]
+ 100
+ 150
+ 200
— 100
— 150
— 200
ADP/(ATP+ADP) on DnaA [%]
DNA [pmol]
D
150 mM NaCl
datA
Structure
+ SC
+ Lin
— SC
— Lin
ADP/(ATP+ADP) on DnaA [%]
DNA [pmol]
E
150 mM NaCl
datA
Structure
+ SC
+ Lin
— SC
— Lin
ADP/(ATP+ADP) on DnaA [%]
Time [min]
F
150 mM NaCl
datA
Structure
+ SC
+ Lin
— SC
— Lin
ADP/(ATP+ADP) on DnaA [%]
IHF [pmol]

Figure 6

A

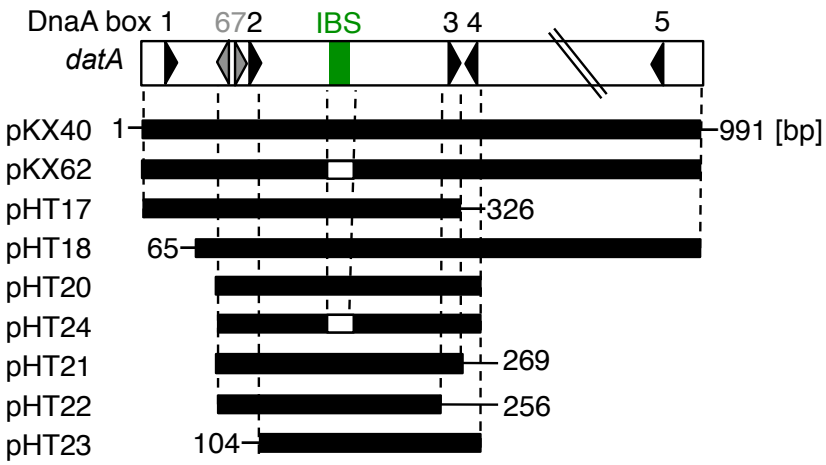

SC, 150 mM NaCl

Plasmid	*datA*	ADP/(ATP+ADP) on DnaA [%]
pKX40	WT	93 ± 7
pKX62	ΔIBS	14 ± 4
pHT17	del2	92 ± 0
pHT18	del3	94 ± 2
pHT20	del5	92 ± 4
pHT24	del5ΔIBS	12 ± 5
pHT21	del6	83 ± 7
pHT22	del7	11 ± 4
pHT23	del8	7.2 ± 0.5
pACYC177	None	6.4 ± 1.4

B

SC, 150 mM NaCl

Plasmid	*datA*	ADP/(ATP+ADP) on DnaA [%]
pKX40	WT	92 ± 5
pKX48	subDnaAbox1	93 ± 3
pKX120	subDnaAbox6	97 ± 0
pHT28	subDnaAbox7	8.0 ± 0.5
pKX41	subDnaAbox2	16 ± 9
pKX43	subDnaAbox3	13 ± 5
pKX47	subDnaAbox4	93 ± 3
pKX49	subDnaAbox5	93 ± 0
pKX42	subIBS	31 ± 0
pACYC177	None	8.6 ± 4.0
-	No DNA	7.9 ± 2.9

Figure 7

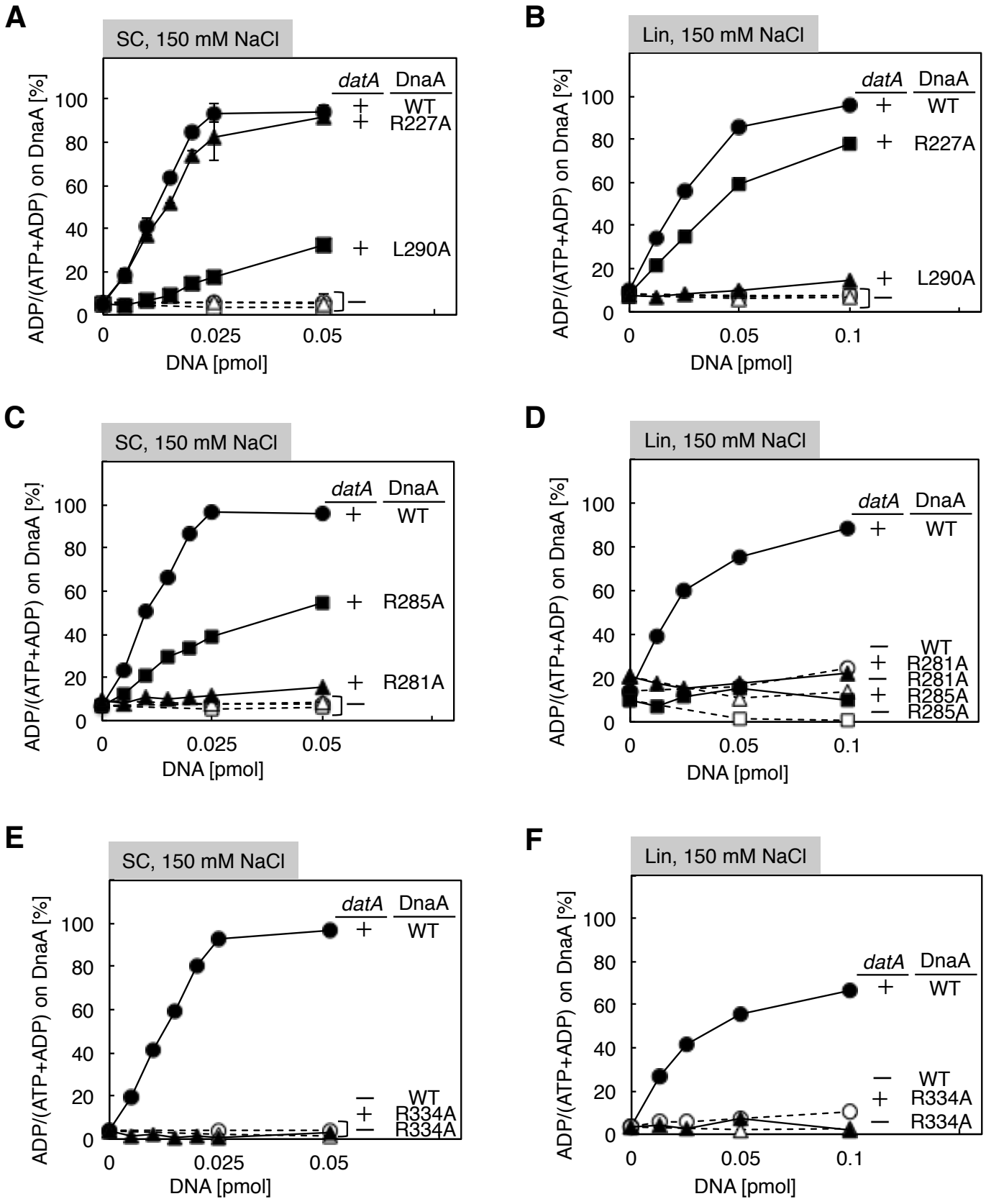
A
SC, 150 mM NaCl
ADP/(ATP+ADP) on DnaA [%]
DNA [pmol]
datA
DnaA
+ WT
+ R227A
+ L290A
− WT
B
Lin, 150 mM NaCl
C
SC, 150 mM NaCl
+ R285A
+ R281A
D
Lin, 150 mM NaCl
− WT
+ R281A
− R281A
+ R285A
− R285A
E
SC, 150 mM NaCl
+ R334A
− R334A
F
Lin, 150 mM NaCl

Figure 8

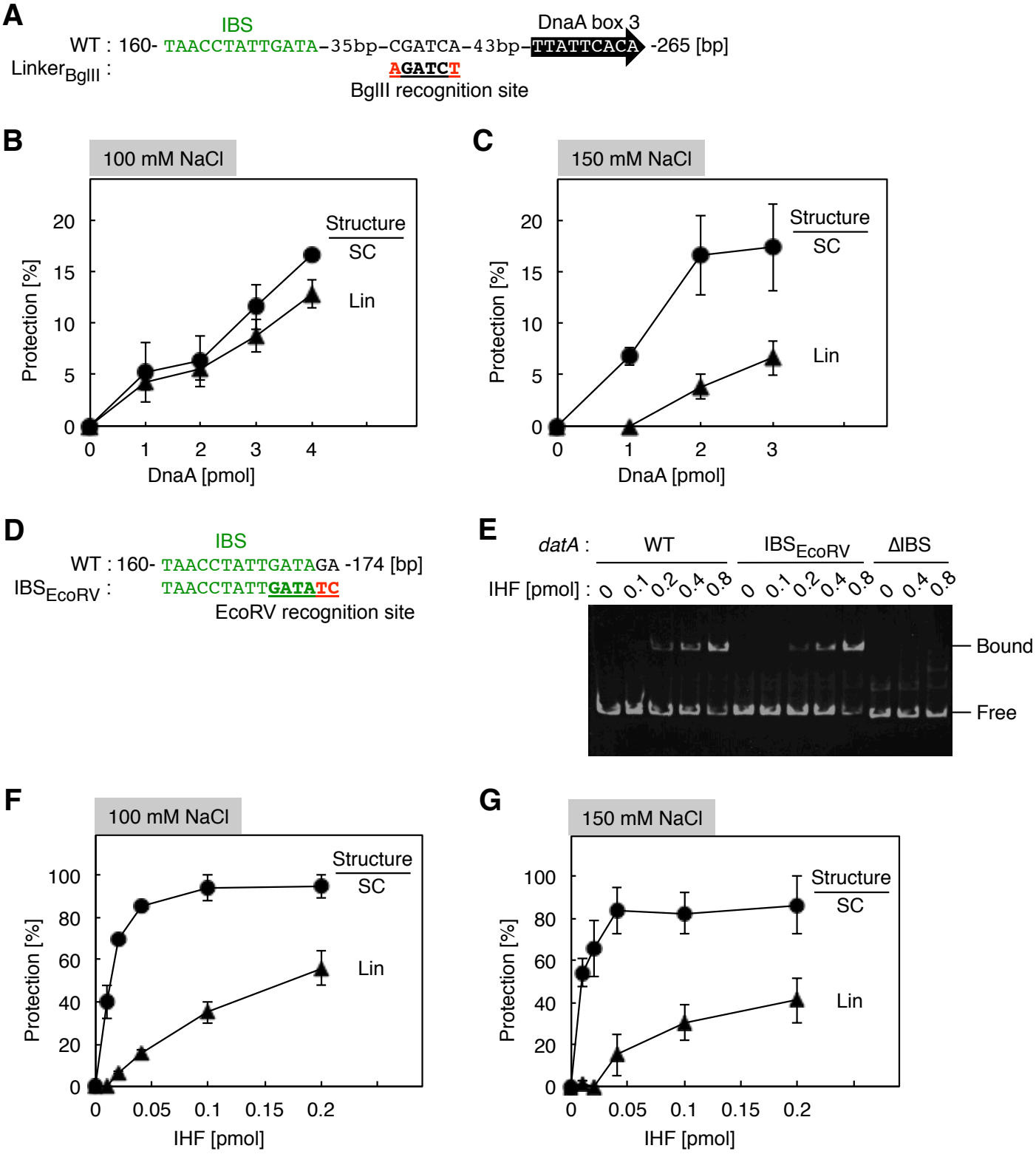
A
IBS
DnaA box 3
WT : 160- TAACCTATTGATA-35bp-CGATCA-43bp-TTATTCACA -265 [bp]
Linker BglII : AGATCT
BglII recognition site
B
100 mM NaCl
Structure
SC
Lin
Protection [%]
DnaA [pmol]
C
150 mM NaCl
Structure
SC
Lin
Protection [%]
DnaA [pmol]
D
IBS
WT : 160- TAACCTATTGATAGA -174 [bp]
IBS EcoRV : TAACCTATTGATATC
EcoRV recognition site
E
datA : WT IBS EcoRV ΔIBS
IHF [pmol] : 0 0.1 0.2 0.4 0.8 0 0.1 0.2 0.4 0.8 0 0.4 0.8
Bound
Free
F
100 mM NaCl
Structure
SC
Lin
Protection [%]
IHF [pmol]
G
150 mM NaCl
Structure
SC
Lin
Protection [%]
IHF [pmol]

Figure 9

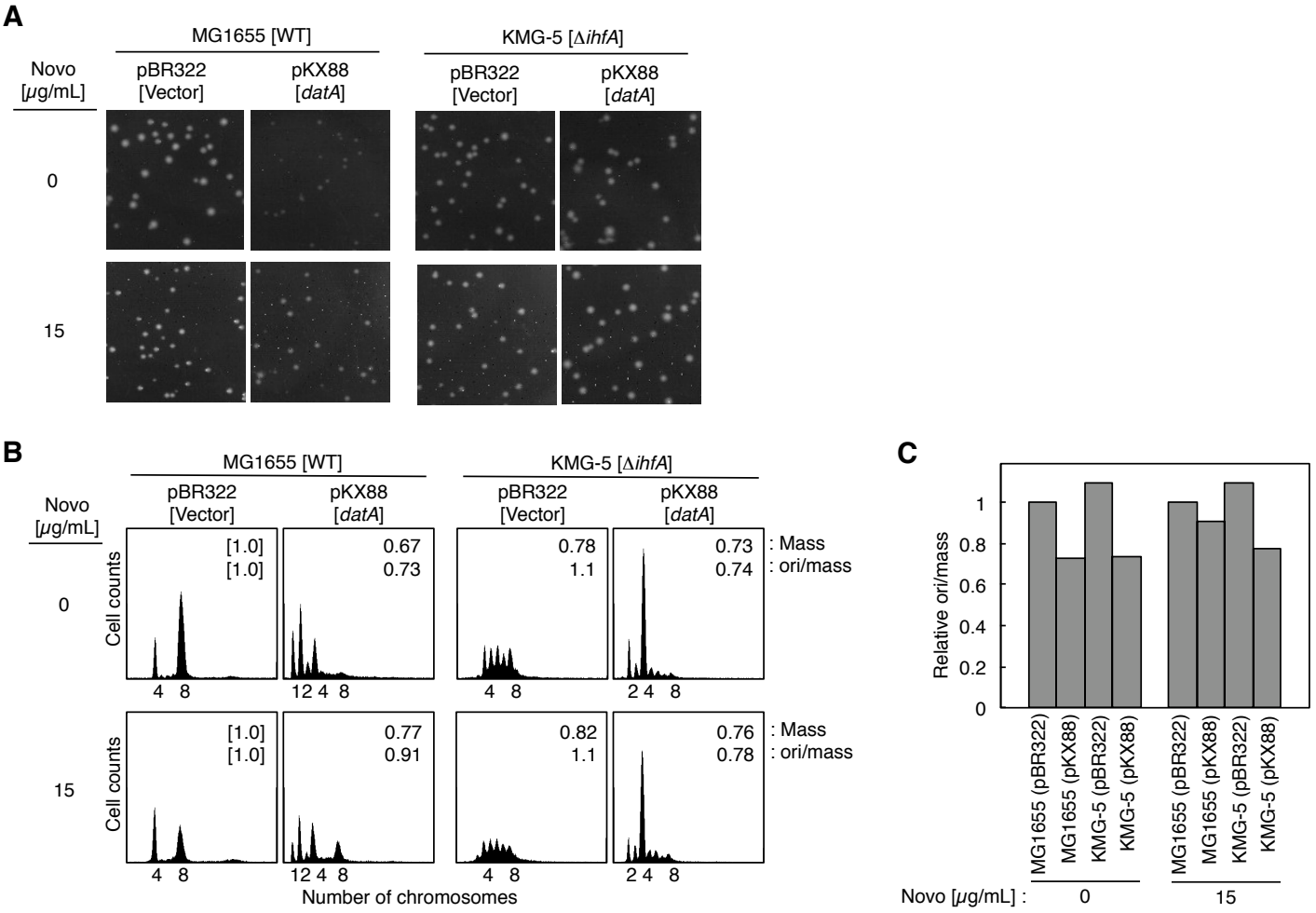

E

Novo [μg/mL]	Relative pBR322/*ter*
0	[1.0]
15	0.97

Figure 10

A

DNA	Requirement of DnaA motifs (residues)				
	Arg-finger (Arg285)	Box VII (Arg281)	Sensor II (Arg334)	AID-1 (Arg227)	AID-2 (Leu290)
oriC	+	+	–	+	+
datA	+	+	+	–	+
DARS1	–	–	–	n.d.	n.d.
DARS2	–	–	–	±	+

B

1. ATP-DnaA oligomer formation
-Inter-ATP-DnaA interaction by Arg285
-Stabilization by Arg281, Leu290, and DNA supercoiling

2. ATPase activation
-Conformational change of DnaA by Arg281
-ATP hydrolysis by Arg334

3. ADP-DnaA dissociation
-Inhibition of inter-DnaA interaction by Leu290

Model. 1
ATP hydrolysis of DnaA on DnaA box 7

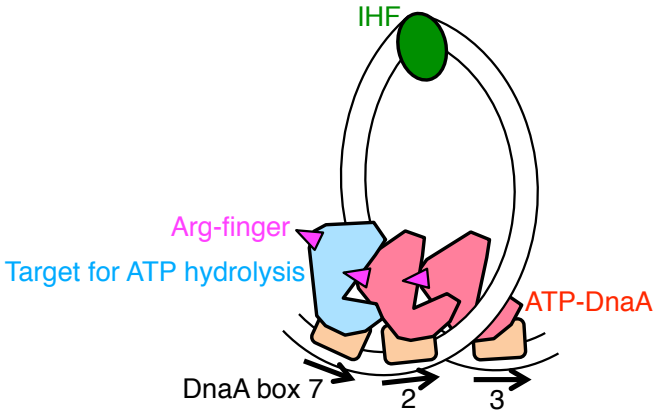

Model. 2
ATP hydrolysis of left DnaA sub-oligomer